Journal of Medicinal Chemistry

Article

pubs.acs.org/jmc

Discovery of 1-[2-Fluoro-4-(1*H*-pyrazol-1-yl)phenyl]-5-methoxy-3-(1-phenyl-1*H*-pyrazol-5-yl)pyridazin-4(1*H*)-one (TAK-063), a Highly Potent, Selective, and Orally Active Phosphodiesterase 10A (PDE10A) Inhibitor

Jun Kunitomo,*[,†] Masato Yoshikawa,[†] Makoto Fushimi,[†] Akira Kawada,[†] John F. Quinn,[‡,§] Hideyuki Oki,[†] Hironori Kokubo,[†] Mitsuyo Kondo,[†] Kosuke Nakashima,[†] Naomi Kamiguchi,[†] Kazunori Suzuki,[†] Haruhide Kimura,[†] and Takahiko Taniguchi[†]

[†]Pharmaceutical Research Division, Takeda Pharmaceutical Company Limited, 26-1, Muraoka-Higashi 2-chome, Fujisawa, Kanagawa 251-8555, Japan

[‡]Albany Molecular Research Inc., 26 Corporate Circle, Albany, New York 12203, United States

Supporting Information

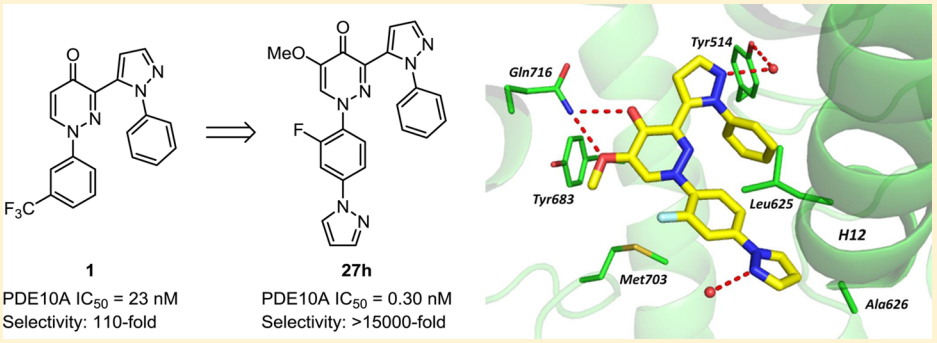

ABSTRACT: A novel series of pyridazinone-based phosphodiesterase 10A (PDE10A) inhibitors were synthesized. Our optimization efforts using structure-based drug design (SBDD) techniques on the basis of the X-ray crystal structure of PDE10A in complex with hit compound **1** (IC_{50} = 23 nM; 110-fold selectivity over other PDEs) led to the identification of 1-[2-fluoro-4-(1*H*-pyrazol-1-yl)phenyl]-5-methoxy-3-(1-phenyl-1*H*-pyrazol-5-yl)pyridazin-4(1*H*)-one (**27h**). Compound **27h** has potent inhibitory activity (IC_{50} = 0.30 nM), excellent selectivity (>15000-fold selectivity over other PDEs), and favorable pharmacokinetics, including high brain penetration, in mice. Oral administration of compound **27h** to mice elevated striatal 3′,5′-cyclic adenosine monophosphate (cAMP) and 3′,5′-cyclic guanosine monophosphate (cGMP) levels at 0.3 mg/kg and showed potent suppression of phencyclidine (PCP)-induced hyperlocomotion at a minimum effective dose (MED) of 0.3 mg/kg. Compound **27h** (TAK-063) is currently being evaluated in clinical trials for the treatment of schizophrenia.

INTRODUCTION

Phosphodiesterases (PDEs) are a superfamily of enzymes that degrade phosphodiester bonds of the intracellular second messenger molecules 3′,5′-cyclic adenosine monophosphate (cAMP) and 3′,5′-cyclic guanosine monophosphate (cGMP).[1] Both cAMP and cGMP mediate biological responses to various extracellular signals and regulate various functions within subcellular domains.[2] Inhibition of PDE can prolong or enhance the effects of physiological processes mediated by cAMP and/or cGMP by inhibiting their degradation. Thus, PDE inhibitors are promising targets for the development of various therapeutic agents.[3]

PDEs are classified into 11 distinct families (PDEs 1−11) on the basis of amino acid sequences, substrate specificities, and pharmacological properties.[1] Each family member is encoded by 1−4 distinct genes and 21 different gene combinations have been reported in mammals. Depending on the organs and tissues where PDE is expressed, a therapeutic agent that inhibits a specific PDE will have different therapeutic implications. PDE10A was originally isolated and characterized as a single member of the dual substrate (cAMP/cGMP) gene family in 1999.[4−6] PDE10A is predominantly expressed in medium spiny neurons of the striatum.[7,8] The striatum is the main input station of the basal ganglia and is strongly associated with motor and cognitive functions.[9,10] Medium spiny neurons integrate synaptic information from midbrain and cortical regions. Thus, PDE10A inhibition may be a promising approach for the treatment of diseases that are related to dysfunctions of the basal ganglia, particularly schizophrenia and Huntington's disease.[11,12] Accordingly,

Received: September 4, 2014

   dx.doi.org/10.1021/jm5013648 | *J. Med. Chem.* XXXX, XXX, XXX−XXX

a number of companies have investigated various PDE10A inhibitors.[12] Of these, PF-2545920 (MP-10),[13] OMS824, RG7203, and FRM-6308 (formerly EVP-6308) are currently being evaluated in clinical trials for the treatment of neurological disorders and psychiatric diseases.

We performed high-throughput screening (HTS) using our proprietary compound library to search for PDE10A inhibitors and identified a pyridazinone derivative **1** with an IC_{50} value of 23 nM and 110-fold selectivity over other PDEs (Figure 1).

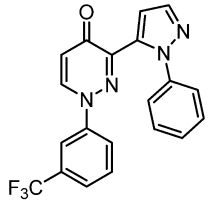

Figure 1. HTS hit compound **1**.

Examination of the X-ray crystal structure of PDE10A in complex with compound **1** indicated the following critical properties (Figure 2): (i) the carbonyl oxygen atom on the pyridazinone ring forms a hydrogen bond with NH of the conserved Gln716 side chain, (ii) the N2 nitrogen atom of the pyrazole ring forms a water-mediated interaction with OH of Tyr514, (iii) the pyridazinone ring makes face-to-face and edge-to-face $\pi-\pi$ stacking interactions with the phenyl rings of Phe719 and Phe686 residues, respectively, (iv) the 3-(trifluoromethyl)phenyl group fits into a hydrophobic region defined by the side chains of Leu625 and Met703 residues, resulting in a twist between the pyridazinone ring and the 3-(trifluoromethyl)phenyl group, and (v) a large unoccupied space lies on the outer side of the 4-position of the 3-(trifluoromethyl)phenyl group. Despite reasonably high selectivity, compound **1** did not bind in the PDE10A selectivity pocket[13] around Tyr683, which is known to enhance potency and selectivity of other PDE10A inhibitors.[13−23]

Applying structure-based drug design (SBDD) on the basis of the crystal structure of compound **1** bound to the PDE10A

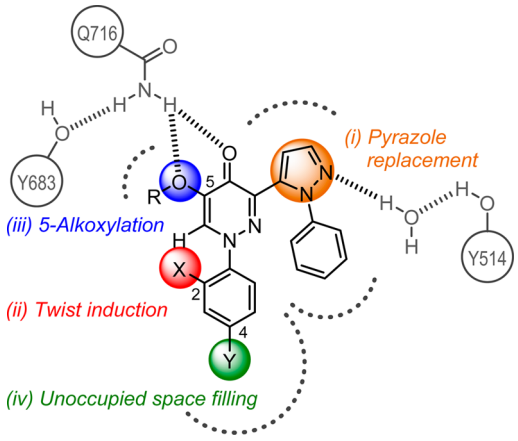

Figure 3. Optimization strategies using SBDD techniques.

catalytic domain, we used the following strategies to optimize subsequent compounds (Figure 3): (i) pyrazole replacement with other heteroaromatic rings carrying a hydrogen-bond acceptor (HBA) that interacts with the Tyr514-bound water molecule, (ii) *o*-substitution on the pendant phenyl group of the pyridazinone ring to produce a twist between the pyridazinone ring and its pendant phenyl group similar to that of the active conformation, (iii) alkoxy introduction at the 5-position of the pyridazinone ring to produce a bidentate interaction with NH of Gln716, and (iv) *p*-substitution on the pendant phenyl group of the pyridazinone ring to effectively fill the unoccupied outer space. In this study, we report structure−activity relationship (SAR) studies of this series and the discovery of 1-[2-fluoro-4-(1*H*-pyrazol-1-yl)phenyl]-5-methoxy-3-(1-phenyl-1*H*-pyrazol-5-yl)pyridazin-4(1*H*)-one (TAK-063, **27h**).

RESULTS AND DISCUSSION

Several PDE10A inhibitors reportedly interact with OH of the Tyr514 side chain through a water-mediated hydrogen bond.[15,24,25] The crystal structure of hit compound **1** with PDE10A revealed that the N2 nitrogen atom of the pyrazole ring forms a hydrogen-bonding interaction with Tyr514 via a water molecule as well (Figure 2), suggesting that other heteroaromatic rings with an HBA corresponding to the N2 nitrogen atom of the

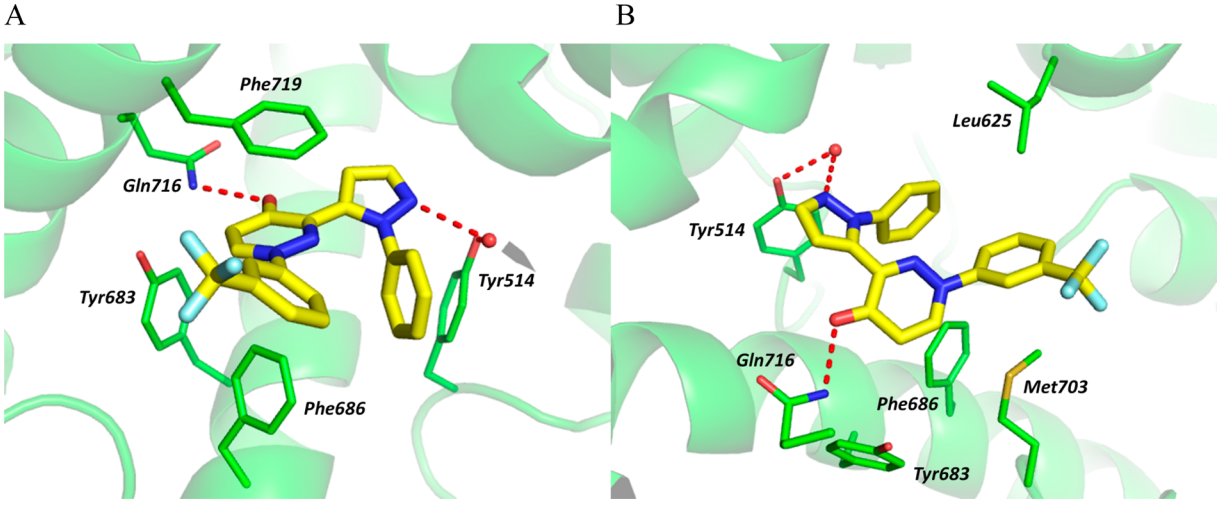

Figure 2. X-ray crystal structures of compound **1** in the PDE10A catalytic domain. (A) Front perspective view. Leu625 and Met703 were omitted for simplicity. (B) Left perspective view. Phe719 was omitted for simplicity.

dx.doi.org/10.1021/jm5013648 | J. Med. Chem. XXXX, XXX, XXX−XXX

Table 1. Pyrazole Replacements

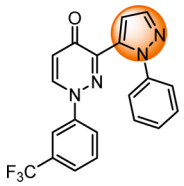

compd	ring	PDE10A IC_{50}[a] (nM)
1		23 (16–34)
11a		2000 (1200–3400)
11b		160 (120–230)
11c		6100 (3300–11000)
11d		480 (410–560)

[a]IC_{50} values and 95% confidence intervals (given in parentheses) were calculated by nonlinear regression analysis of percent inhibition data (n = 2). All values were rounded to two significant digits.

pyrazole ring might bind to the Tyr514-bound water molecule with higher affinity. Thus, a series of pyrazole ring replacements were investigated (Table 1). Among these, the triazole analogue **11a** showed markedly reduced potency compared with the pyrazole analogue **1**. The increase of desolvation penalty due to the N4 nitrogen atom of the triazole ring is the most likely cause of this loss of activity. The imidazole analogue **11b** had 7-fold weaker potency than the pyrazole analogue **1**, presumably reflecting the influence of alterations in electron density or the basicity of the HBA. Loss of potency was also observed for furan and six-membered pyridine analogues **11c** and **11d**, indicating that the hydrogen bonding interaction with Tyr514 is weakened due to the change of the lone-pair orientation of the HBA. Accordingly, the pyrazole ring was identified as the most suitable heteroaromatic ring for the water-mediated interaction with Tyr514.

The pendant phenyl group on the pyridazinone ring fitted closely into the hydrophobic region between Leu625 and Met703 residues, causing a moderate twist between the pyridazinone ring and its pendant phenyl group (Figure 2). Twist induction by *o*-substitution on the pendant phenyl group was expected to improve potency due to easy conversion to the active conformation. Hence, the effects of *o*-substituents of various sizes were evaluated (Table 2). *o*-Trifluoromethylation (**14a**) resulted in a significant loss of activity. Potency was recovered with decreasing sizes of the *o*-substituents, but the potency of *o*-fluoro and *o*-unsubstituted analogues **14d** and **14e** remained comparable to that of hit compound **1**. Unexpectedly, these data demonstrate that the forced twist has a negative effect on the formation of the active conformation, and only fluorine and hydrogen atoms at the *o*-position led to potent compounds. Although selectivity of the two analogues was comparable, the *o*-fluoro analogue **14d** had greater metabolic stability than the *o*-unsubstituted analogue **14e**, presumably reflecting the electron-withdrawing effect of the fluorine atom.

Table 2. *o*-Substitution on the Pendant Phenyl Group

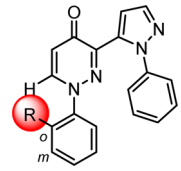

compd	R	PDE10A IC_{50}[a] (nM)	PDE10A selectivity[b]	HLM[c] (μL/min/mg)
14a	CF_3	>1000	nt[d]	<1
14b	Me	940 (630–1400)	nt[d]	38
14c	Cl	120 (100–150)	nt[d]	36
14d	F	33 (11–99)	>300[e]	<1
14e	H	18 (12–27)	>560[e]	16

[a]IC_{50} values and 95% confidence intervals (given in parentheses) were calculated by nonlinear regression analysis of percent inhibition data (n = 2). All values were rounded to two significant digits. [b]Minimum selectivity (rounded to two significant digits) over other PDEs. [c]Metabolic stability in human liver microsomes. [d]Not tested. [e]IC_{50} > 10 μM for other PDEs.

Compound **14e**, which is an *m*-unsubstituted analogue of compound **1**, exhibited >5-fold higher selectivity than compound **1** due to lowered activity against other PDEs (IC_{50} > 10 μM). The *o*-fluoro analogue **14d** also had IC_{50} values of >10 μM for other isoforms, resulting in enhanced PDE10A selectivity compared with compound **1**. Compounds with an *m*-unsubstituted pendant phenyl ring were most likely to have improved PDE10A selectivity and had lower molecular weights. Thus, the *m*-position remained unsubstituted in subsequent optimized compounds.

Modification of the pyridazinone moiety in hit compound **1** was performed in parallel with the SAR study of the pendant phenyl ring. Accordingly, particular attention was given to the crystal structures of ligands that form a bidentate hydrogen-bonding interaction with NH of Gln716.[14,26−28] Specifically, the crystal structure of papaverine bound to the PDE10A catalytic domain indicated that two methoxy groups of the isoquinoline ring shared the hydrogen-bond donor NH of Gln716 (Figure 4).[26] Comparison of the crystal structure of compound **1** with that of papaverine gave rise to the idea that introduction of an alkoxy group at the 5-position of the pyridazinone ring, which corresponds to the position of the 7-methoxy group on the isoquinoline ring in papaverine, would provide further improved activity. As anticipated, the 5-methoxy analogue **20a** was approximately 16-fold more potent than compound **1**, with a nanomolar IC_{50} value (Table 3). In contrast, the 5-hydroxy analogue **20b** had dramatically reduced potency compared with compound **1**, presumably reflecting the formation of an intramolecular hydrogen bond between the hydroxy group and the vicinal carbonyl oxygen atom and interrupting the interaction between the carbonyl oxygen atom and the Gln716 side chain. Conversion of methoxy to difluoromethoxy (**20c**), ethoxy (**20d**), or isopropoxy (**20e**) also reduced potency and lowered corresponding selectivity with increasing sizes of the alkyl moieties. Compared with the methoxy group, the bulky alkoxy groups likely caused steric repulsion with the amino acids located close to the 5-position of the pyridazinone ring. In the case of the difluoromethoxy analogue **20c**, the increase of desolvation penalty due to its higher polarity could possibly also affects the loss of potency.

To investigate the significance of the methoxy group in compound **20a**, we performed X-ray crystal structure analysis of

dx.doi.org/10.1021/jm5013648 | J. Med. Chem. XXXX, XXX, XXX−XXX

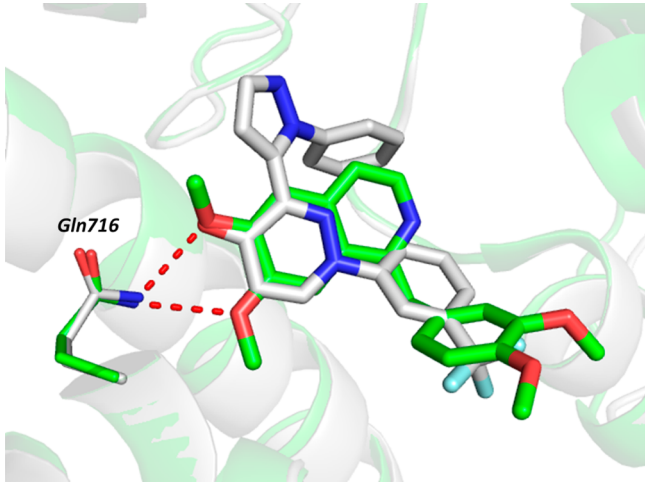

Figure 4. Overlaid crystal structures of papaverine (green, PDB ID 2WEY) and compound **1** (white) in the PDE10A catalytic domain. The bidentate interaction between NH of the Gln716 side chain and two methoxy groups of the isoquinoline ring in papaverine is highlighted with red dashed lines.

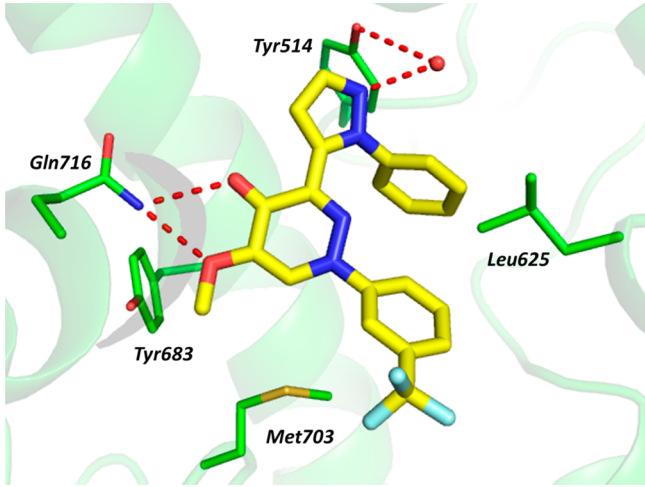

Figure 5. X-ray crystal structure of compound **20a** in the PDE10A catalytic domain. The bidentate interaction between NH of the Gln716 side chain and the 5-methoxypyridazinone ring is highlighted with red dashed lines. Phe719 and Phe686 formed $\pi-\pi$ interactions with the pyridazinone ring but were omitted for simplicity.

Table 3. C5-Alkoxylation on the Pyridazinone Ring

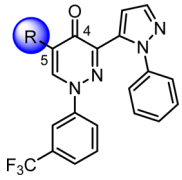

		PDE10A	
compd	R	IC_{50}[a] (nM)	selectivity[b]
1	H	23 (16–34)	110
20a	OMe	1.4 (1.3–1.5)	180
20b	OH	>10000	nd[c]
20c	$OCHF_2$	130 (85–200)	10
20d	OEt	59 (43–81)	25
20e	O*i*-Pr	820 (640–1100)	0.60

[a]IC_{50} values and 95% confidence intervals (given in parentheses) were calculated by nonlinear regression analysis of percent inhibition data (n = 2). All values were rounded to two significant digits. [b]Minimum selectivity (rounded to two significant digits) over other PDEs. [c]Not determined because of IC_{50} values of >10 μM for all PDEs.

PDE10A in complex with compound **20a** (Figure 5). The methoxy oxygen atom accepted an additional hydrogen bond from NH of the Gln716 side chain, resulting in an effective predicted bidentate interaction between the pyridazinone moiety and Gln716. Furthermore, the methoxy group was of a suitable size to fit into the space around the 5-position of the pyridazinone ring. This crystal structure successfully explains why the 5-methoxy analogue **20a** had the highest potency among the compounds listed in Table 3.

The crystal structures of compounds **1** and **20a** in the PDE10A catalytic domain demonstrated considerable open space on the outer side of the 4-position of the pendant phenyl group (Figures 2 and 5). Filling of the unoccupied space offered the potential for a significant increase in PDE10A potency and consequent improvement of selectivity. Thus, a diverse set of substitutions at the 4-position of the pendant phenyl group were investigated in 1-(2-fluorophenyl)-5-methoxy-3-(1-phenyl-1*H*-pyrazol-5-yl)pyridazin-4(1*H*)-ones carrying the most favorable parts identified in the above SAR studies (Table 4). The 2-fluoro-4-unsubstituted analogue **27a** exhibited unexpectedly low potency compared with the corresponding 3-trifluoromethyl analogue **20a**. Nonetheless, the selectivity of compound **27a** was enhanced approximately 4-fold compared with that of compound **20a**. Moreover, 4-trifluoromethylation (**27b**) and 4-trifluoromethoxylation (**27c**) on the pendant phenyl group in compound **27a** led to 2- and 4-fold increases in potency, respectively, with nanomolar IC_{50} values. The trifluoromethoxy analogue **27c** displayed approximately 2700-fold selectivity, which was several-fold superior to the unsubstituted and trifluoromethyl analogues **27a** and **27b**, suggesting that larger substituents increase both potency and selectivity. Replacement with more bulky morpholine (**27d**) led to a remarkable increase in potency, with a subnanomolar IC_{50} value, and consequent selectivity. However, unlike compounds **27a–c**, the morpholine analogue **27d** displayed poor in vitro metabolic stability in human hepatic microsomes, potentially reflecting oxidative metabolism of the morpholine moiety. The oxidized morpholinone analogue **27e** exhibited better metabolic stability than the morpholine analogue **27d** but had 10-fold lower potency and a markedly increased efflux ratio in P-glycoprotein (P-gp)-overexpressing cells. High efflux ratio was also observed in experiments with the oxazolidinone analogue **27f**, presumably due to a large topological polar surface area (TPSA) value[29] (91 Å^2) that was similar to that of compound **27e**. However, the associated ring contraction improved both potency and metabolic stability. These observations suggest that imidazole and pyrazole rings, which are 5-membered heteroaromatic rings with reduced TPSA values, are potential substituents that satisfy both good metabolic stability and favorable efflux ratios without losing potency and selectivity. Both imidazole and pyrazole analogues **27g** and **27h** displayed marked potency, with subnanomolar IC_{50} values, and >10000-fold selectivity. These compounds also exhibited desirable metabolic stability in human microsomes (<10 μL/min/mg) and had acceptable TPSA values (80 Å^2). Despite having similar TPSA values, the efflux ratio of the imidazole analogue **27g** was as high as that of morpholinone and oxazolidinone analogues **27e** and **27f**, whereas that of the pyrazole analogue **27h** was significantly better (0.7). This

dx.doi.org/10.1021/jm5013648 | J. Med. Chem. XXXX, XXX, XXX–XXX

Table 4. C4-Substitution on the Pendant Phenyl Group in 5-Methoxy-3-(1-phenyl-1*H*-pyrazol-5-yl)pyridazin-4(1*H*)-ones

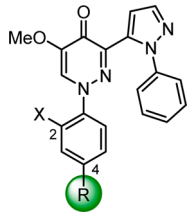

			PDE10A		HLM[c]	TPSA[d]	
compd	R	X	IC_{50}[a] (nM)	selectivity[b]	(μL/min/mg)	(Å^2)	ER[e]
27a	H	F	12 (8.9–16)	780	<1	62	0.7
27b	CF_3	F	5.5 (3.6–8.5)	670	<1	62	0.5
27c	OCF_3	F	3.0 (2.1–4.3)	2700	<1	71	0.4
27d		F	0.38 (0.27–0.54)	6300	123	74	1.2
27e		F	4.0 (2.7–5.9)	>2500[f]	37	91	7.4
27f		F	0.94 (0.72–1.2)	4600	<1	91	6.2
27g		F	0.20 (0.15–0.27)	30000	6	80	7.0
27h		F	0.30 (0.22–0.40)	18000	4	80	0.7
35		H	0.11 (0.078–0.14)	15000	151	80	1.5

[a]IC_{50} values and 95% confidence intervals (given in parentheses) were calculated by nonlinear regression analysis of percent inhibition data (n = 2 or 3). All values were rounded to two significant digits. [b]Minimum selectivity (rounded to two significant digits) over other PDEs. [c]Metabolic stability in human liver microsomes. [d]Calculated using Daylight. [e]MDR1 efflux ratios in P-gp-overexpressing cells. [f]IC_{50} > 10 μM for other PDEs.

discrepancy may be due to nitrogen atoms on introduced heteroaromatic rings. Specifically, the basic N3 nitrogen atom of the imidazole ring is exposed to the surface of the molecule in compound **27g**, whereas the N2 nitrogen atom of the pyrazole ring is masked inside the molecule in compound **27h**. These data indicate that the pyrazole ring is the most desirable substituent at the 4-position of the pendant phenyl ring. Because a hydrogen atom at the 2-position of the pendant phenyl ring was an alternative with high potency (Table 2), we confirmed the potential of the 2-unsubstituted pendant phenyl analogue of compound **27h** (compound **35**) as a drug candidate. However, removal of the fluorine atom from compound **27h** resulted in marked loss of metabolic stability (151 μL/min/mg) despite retention of remarkable potency and high selectivity. As with the data presented in Table 2, the electron-withdrawing fluorine atom in compound **27h** is considered to protect the pendant phenyl moiety against the metabolic liabilities arising from introduction of the pyrazole ring.

The crystal structure of compound **27h** bound to PDE10A is illustrated in Figure 6. As with the crystal structures of PDE10A complex with compounds **1** and/or **20a**, $\pi-\pi$ stacking interactions (not shown in the figure) and a bidentate hydrogen-bonding interaction in the pyridazinone moiety were observed, and the N2 nitrogen atom of the pyrazole ring formed a water-mediated interaction with OH of Tyr514 as well. In addition, the

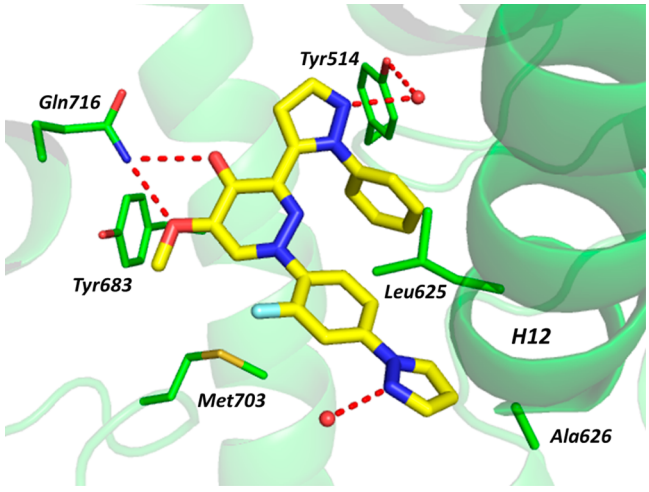

Figure 6. X-ray crystal structure of compound **27h** in the PDE10A catalytic domain. Phe719 and Phe686 formed $\pi-\pi$ interactions with the pyridazinone ring but were omitted for simplicity.

pyrazole ring on the pendant phenyl group effectively fills the large space adjacent to the Leu625 and Ala626 residues at the N-terminus of helix H12[30] along with a hydrogen-bonding interaction with a water molecule located close to the N2

dx.doi.org/10.1021/jm5013648 | J. Med. Chem. XXXX, XXX, XXX−XXX

nitrogen atom. The present SBDD strategies produced compounds with extremely potent inhibitory activity and excellent selectivity for PDE10A, with a unique binding mode that is distinct from that of previously characterized PDE10A inhibitors.[11]

In addition to excellent PDE10A selectivity (Table 5), compound **27h** exhibited only slight activity (<50% at 10 μM) against 91 receptors, ion channels, and enzymes (except for 5 PDEs) in an MDS Pharma Services (now Ricerca Biosciences) screen, which was performed to assess potential off-target activities. Moreover, compound **27h** showed high oral absorption and brain penetration (Kp_{brain} = 1.64) in mice, and the mean residence time (MRT) in the brain were suggestive of long-lasting efficacy of this compound (Table 6). In light of in vitro and pharmacokinetic data, we selected compound **27h** for further evaluation in animal models of schizophrenia.

Table 5. Inhibitory Activities of Compound 27h against Human PDEs

isoform	IC_{50}[a] (nM)
PDE1A	12000 (9800−14000)
PDE2A3	>30000
PDE3A	>30000
PDE4D2	5500 (5000−6100)
PDE5A1	5700 (4700−6900)
PDE6AB	6800 (5300−8900)
PDE7B	19000 (18000−21000)
PDE8A1	>30000
PDE9A2	>30000
PDE10A2	0.30 (0.22−0.40)
PDE11A4	>30000

[a]IC_{50} values and 95% confidence intervals (given in parentheses) were calculated by nonlinear regression analysis of percent inhibition data (n = 3). All values were rounded to two significant digits.

Table 6. Pharmacokinetic Parameters of Compound 27h in Mice[a]

	plasma	brain
C_{max} (μg/mL or μg/g)	0.104	0.097
T_{max} (h)	1.00	2.00
AUC_{0-24h} (μg·h/mL or μg·h/g)	0.650	1.066
MRT[b] (h)	4.64	7.21
Kp_{brain}[c]		1.64

[a]Administered orally at 0.3 mg/kg (n = 3). [b]Mean residence time. [c]Brain-to-plasma AUC_{0-24h} ratio.

Because PDE10A is a dual substrate (cAMP/cGMP) enzyme and is abundantly expressed in the striatum, the effects of compound **27h** on striatal cyclic nucleotide levels were evaluated in mice. As shown in Figure 7, oral administration of compound **27h** at 0.3 mg/kg to ICR mice significantly increased striatal cAMP and cGMP levels by 1.30-fold to 1.60 pmol/mg tissue and 2.14-fold to 0.11 pmol/mg tissue, respectively.

Subsequently, we evaluated the potential antipsychotic-like effects of compound **27h** in mice demonstrating phencyclidine (PCP)-induced hyperlocomotion, an established rodent model of acute schizophrenic psychosis.[31,32] Compound **27h** was administered orally to C57BL/6 male mice at doses of 0.1, 0.3, or 1.0 mg/kg 60 min before PCP treatment (5 mg/kg as a salt, sc). Compound **27h** significantly reversed the PCP-induced hyperlocomotion in a dose-dependent manner, with a minimum effective dose (MED) of 0.3 mg/kg, po (Figure 8A). In contrast, compound **27h** had no effects on the hyperactivity produced by PCP in PDE10A-knockout (KO) mice at doses of up to 1 mg/kg, po (Figure 8B). These data provide strong evidence that the antipsychotic-like effects of compound **27h** reflect PDE10A inhibition and subsequent increases in striatal cAMP and cGMP levels.

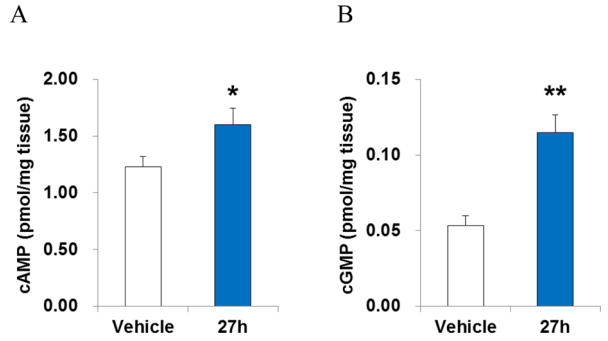

Figure 7. Elevation of mouse striatal cAMP (A) and cGMP (B) levels 60 min after oral administration of compound **27h** at 0.3 mg/kg to ICR mice. Data are presented as the mean ± SEM (n = 12); *$p \leq 0.05$, **$p \leq 0.01$ vs vehicle; Aspin−Welch test.

CHEMISTRY

Pyrazole replacements were performed as shown in Scheme 1. Diazotization of the aniline **2** with $NaNO_2$ and HCl aq followed by treatment with methyl acetoacetate afforded the hydrazone **3**. Heating of **3** in *N*,*N*-dimethylformamide dimethyl acetal (DMFDMA) yielded the pyridazinone **4**. Direct amidation of the ester of **4** and subsequent heating of **5** in DMFDMA produced the dimethylaminomethylene **6**. Cyclization of **6** with phenylhydrazine afforded the triazole analogue **11a**. The ester of **4** was hydrolyzed to the carboxylic acid **7**, which was converted to the amine **8** via Curtius rearrangement. Treatment of **8** with glyoxal followed by reaction with benzaldehyde and NH_4Cl yielded the imidazole analogue **11b**. Sandmeyer reaction of **8** using $CuBr_2$ afforded the bromide **9**. Suzuki−Miyaura coupling of **9** with (2-phenyl-3-furyl)boronic acid and (2-chloropyridin-3-yl)boronic acid produced the furan analogue **11c** and the chloropyridine intermediate **10**, respectively. The intermediate **10** was subjected to Suzuki−Miyaura coupling with phenylboronic acid to afford the pyridine analogue **11d**.

Scheme 2 shows the protocol for the synthesis of compounds **14a−e** with a 2-substituted pendant phenyl group. Diazotization of anilines **12a−e** followed by treatment with acetylacetone yielded hydrazones **13a−e**. Heating of compounds **13a−e** in DMFDMA and subsequent cyclization to pyrazole rings afforded the desired products **14a−e**.

The protocol for the preparation of compounds **20a−e** with a 5-alkoxylpyridazinone ring is illustrated in Scheme 3. The ester intermediate **16** was prepared in a manner similar to that described in Scheme 1. Conversion of **16** to the Weinreb amide **17** and subsequent Grignard reaction with methylmagnesium bromide afforded the methyl ketone **18**. Application of the same reactions shown in Scheme 2 to **18** gave the 5-methoxypyridazinone **20a**. Demethylation of **20a** using NaI and trimethylsilyl chloride (TMSCl)[33] yielded the 5-hydroxy analogue **20b**. Alkylation of **20b** with sodium chlorodifluoroacetate, iodoethane, and 2-iodopropane produced the 5-difluoromethoxy (**20c**), 5-ethoxy (**20d**), and 5-isopropoxy (**20e**) analogues, respectively.

dx.doi.org/10.1021/jm5013648 | J. Med. Chem. XXXX, XXX, XXX−XXX

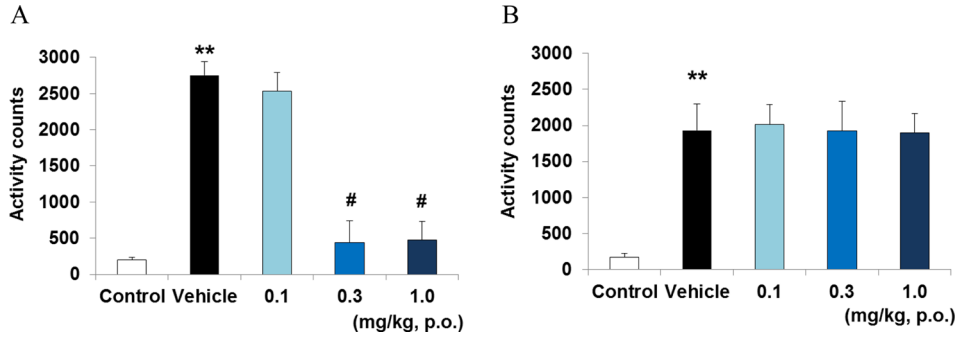

Figure 8. Effects of compound **27h** on PCP-induced hyperlocomotion in mice. PCP (5 mg/kg as a salt) was administered subcutaneously 60 min after oral treatment of C57BL/6 (A) or PDE10A-KO mice (B) with compound **27h**. Accumulated activity counts over 120 min after PCP treatment were recorded and are presented as the mean ± SEM (n = 3−5/group); $^{**}p \leq 0.01$ vs control; Aspin−Welch test; $\#p \leq 0.025$ vs vehicle + PCP; one-tailed Williams' test.

Scheme 1. Synthesis of Compounds 11a−d[a]

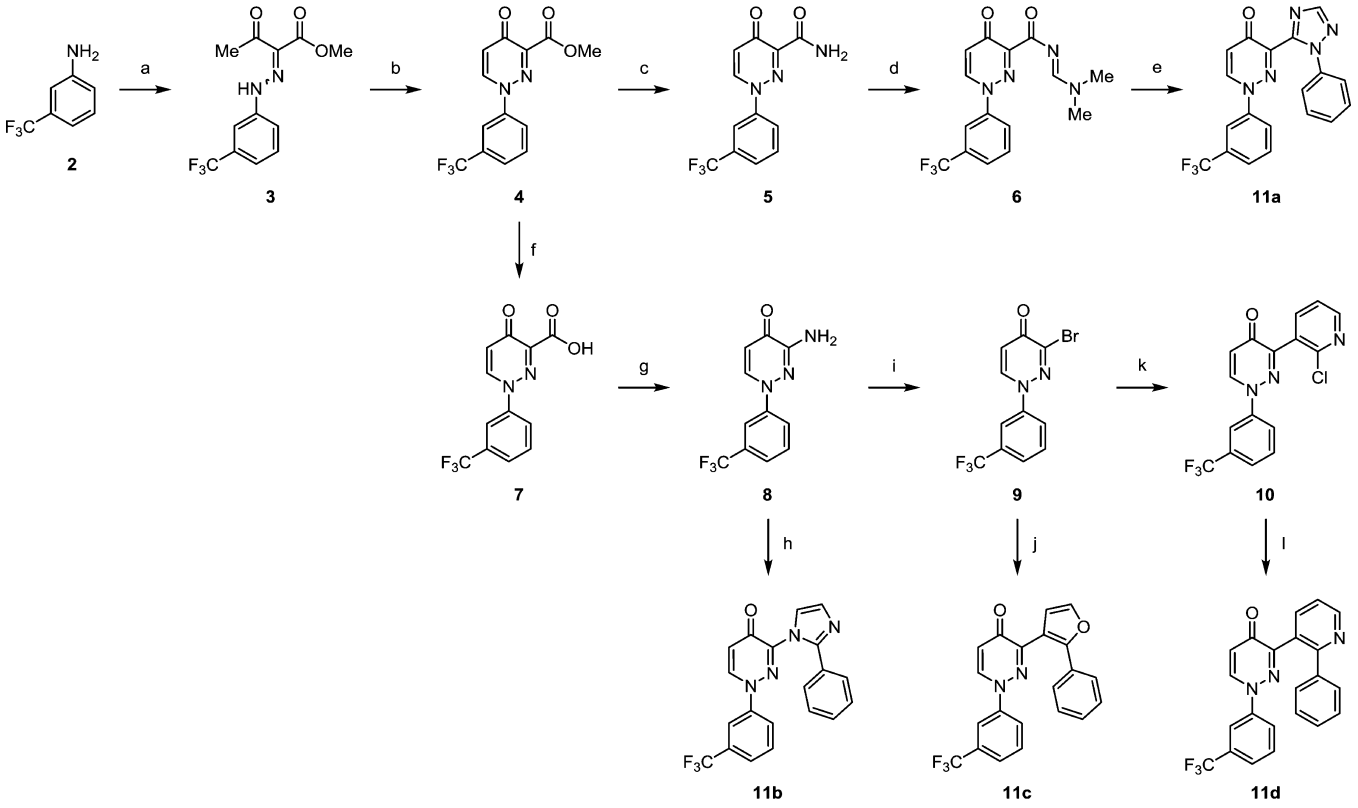

[a]Reagents and conditions: (a) (1) $NaNO_2$, HCl aq, 0 °C, (2) methyl acetoacetate, NaOAc, EtOH, 0 °C, 69%; (b) DMFDMA, reflux, 87%; (c) NH_3, MeOH, microwave, 100 °C, 64%; (d) DMFDMA, microwave, 130 °C, 76%; (e) phenylhydrazine, AcOH, microwave, 120 °C, 94%; (f) NaOH aq, MeOH, rt, 97%; (g) (1) DPPA, Et_3N, toluene, 100 °C, (2) NaOH aq, rt, 56%; (h) (1) glyoxal aq, MeOH, rt, (2) benzaldehyde, NH_4Cl, reflux, (3) H_3PO_4, reflux, 3%; (i) isoamyl nitrite, $CuBr_2$, DMF, 0−60 °C, 82%; (j) (2-phenyl-3-furyl)boronic acid, $Pd(PPh_3)_4$, Na_2CO_3, DME/water, 80 °C, 7%; (k) (2-chloropyridin-3-yl)boronic acid, $Pd(PPh_3)_4$, Na_2CO_3, DME/water, 80−100 °C, 27%; (l) phenylboronic acid, $Pd(PPh_3)_4$, Na_2CO_3, DME/water, 80 °C, 36%.

Scheme 4 describes the synthesis of 1-(2-fluorophenyl)-5-methoxypyridazones **27a−h**. In a manner similar to that shown in Scheme 3, compounds **27a**, **27c**, and the key intermediate **26** were prepared from the corresponding anilines **21a−c**. Copper-catalyzed reaction of **26** with methyl 2,2-fluoro-2-(fluorosulfonyl)-acetate afforded the trifluoromethyl analogue **27b**.[34] The morpholine analogue **27d** was prepared through Buchwald−Hartwig reaction of **26** with morpholine.[35] The morpholinone (**27e**), oxazolidinone (**27f**), and imidazole (**27g**) analogues were obtained by Ullmann-type coupling of **26** with the corresponding heterocycles.[36] Preparation of the pyrazole analogue **27h** was accomplished by copper-catalyzed substitution of **26** with pyrazole in the presence of salicylaldoxime as a ligand.[37]

Synthesis of compound **35** was accomplished as shown in Scheme 5 using a method similar to that described for the synthesis of **27h**. In this instance, the methyl ketone **33** was prepared from the ester **30** via condensation of the carboxylic acid **31** with Meldrum's acid and subsequent decarboxylation of **32** under acidic conditions. The alternative process was also available for preparing the methyl ketone from the corresponding ester.

dx.doi.org/10.1021/jm5013648 | J. Med. Chem. XXXX, XXX, XXX−XXX

Scheme 2. Synthesis of Compounds 14a−e[a]

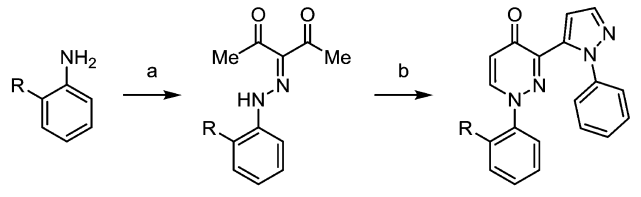

12a: R = CF_3 **13a**: R = CF_3 **14a**: R = CF_3
12b: R = Me **13b**: R = Me **14b**: R = Me
12c: R = Cl **13c**: R = Cl **14c**: R = Cl
12d: R = F **13d**: R = F **14d**: R = F
12e: R = H **13e**: R = H **14e**: R = H

[a]Reagents and conditions: (a) (1) $NaNO_2$, HCl aq, 0 °C, (2) acetylacetone, NaOAc, EtOH/water, rt, 33−67%; (b) (1) DMFDMA, reflux, (2) phenylhydrazine, MeOH, reflux, 7−31%.

CONCLUSION

HTS of our proprietary compound library identified the pyridazinone derivative **1** with an IC_{50} value of 23 nM and 110-fold selectivity over other PDEs. Thus, we performed SAR studies for optimization using SBDD techniques on the basis of the X-ray crystal structure of compound **1** bound to PDE10A. 5-Methoxylation on the pyridazinone ring yielded a remarkable increase in potency. Crystal structure analysis of compound **20a** bound to PDE10A revealed that the 5-methoxy group shares NH of the Gln716 side chain with the vicinal carbonyl group to form a bidentate hydrogen-bonding interaction. Furthermore, introduction of a range of heterocyclic groups at the 4-position on the pendant phenyl group of the pyridazinone ring resulted in remarkable increase in both potency and selectivity. Finally, the present optimization strategy led to the identification of 1-[2-fluoro-4-(1*H*-pyrazol-1-yl)phenyl]-5-methoxy-3-(1-phenyl-1*H*-pyrazol-5-yl)pyridazin-4(1*H*)-one (**27h**), which showed potent activity (IC_{50} = 0.30 nM) and excellent selectivity (>15000-fold selectivity over other PDEs) without exhibiting significant activity against 91 off-target receptors, ion channels, or enzymes (except for PDEs). In subsequent animal studies, compound **27h** provoked a significant increase in levels of both striatal cAMP and cGMP in mice at 0.3 mg/kg, po. Moreover, dose-dependent suppression of PCP-induced hyperlocomotion was observed in mice with an MED of 0.3 mg/kg, po. With potent in vivo efficacy and favorable preclinical pharmacokinetic properties, including high brain penetration, compound **27h** was selected as a drug candidate and is under investigation in clinical trials for the treatment of schizophrenia.

EXPERIMENTAL SECTION

General Chemistry Information. All commercially available solvents and reagents were used without further purification. Yields were not optimized. Melting points were determined on a Büchi melting point apparatus B-545 or an OptiMelt melting point apparatus MPA100 and were not corrected. ^{1}H NMR spectra were recorded on Varian Mercury-300 (300 MHz) or Bruker DPX300 (300 MHz) instruments. Chemical shifts are reported as δ values (ppm) downfield from internal TMS of the indicated organic solution. Peak multiplicities are expressed as follows: s, singlet; d, doublet; t, triplet; q, quartet; dd, doublet of doublets; td, triplet of doublets; ddd, doublet of doublet of doublets; brs, broad singlet; m, multiplet. Coupling constants (J values) are given in hertz (Hz). LC-MS was performed on a Waters liquid chromatography−mass spectrometer system, using a CAPCELL PAK UG-120 ODS column (2.0 mm i.d. × 50 mm, Shiseido Co., Ltd.) with a 5−95% gradient of CH_3CN in water containing 0.04% TFA and an HP-1100 (Agilent Technologies) apparatus for monitoring at 220 nm. All microwave reactions were performed in a Biotage Initiator 2.0 or 2.5 microwave synthesizer. Preparative HPLC was performed on an automated Gilson HPLC system using a YMC C-18 column (S-5 μm, 50 mm × 20 mm i.d.) with a 5−95% gradient of CH_3CN in water containing 0.1% TFA. Reaction progress was determined by TLC analysis on Merck Kieselgel 60 F254 plates or Fuji Silysia NH plates. Column chromatography was performed using silica gel (Merck Kieselgel 60, 70−230 mesh), basic silica gel (Chromatorex NH-DM 1020, 100−200 mesh, Fuji Silysia Chemical, Ltd.), or Purif-Pack (SI ϕ 60 μM or NH ϕ 60 μM, Fuji Silysia Chemical, Ltd.). Element analyses

Scheme 3. Synthesis of Compounds 20a−e[a]

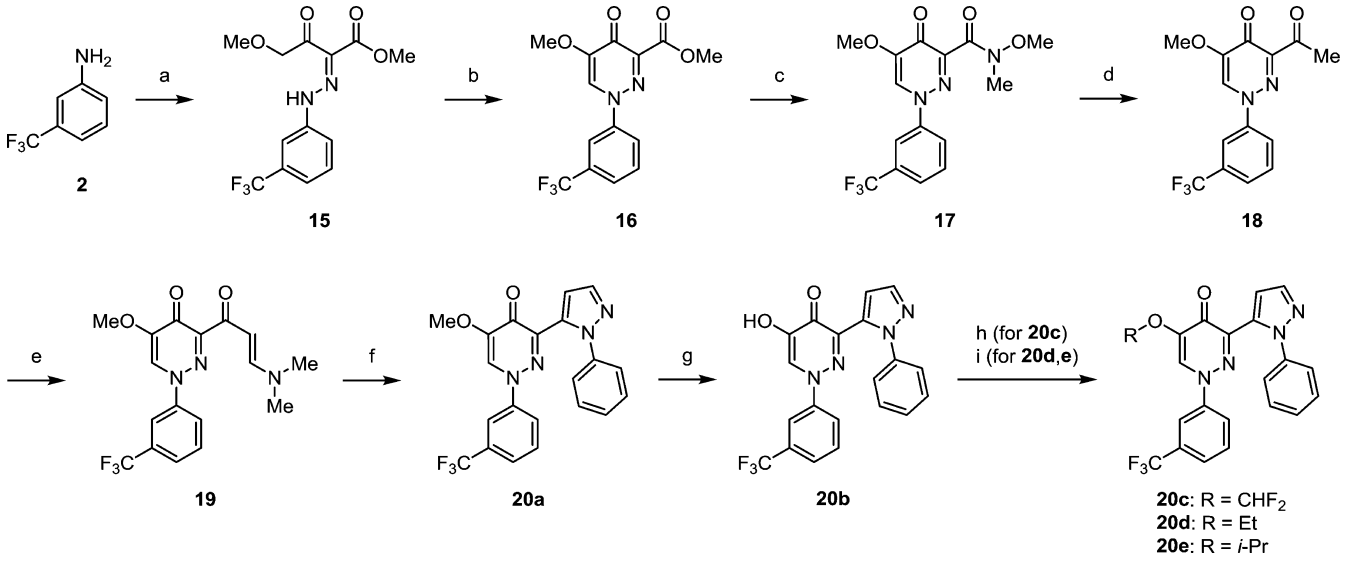

2 **15** **16** **17** **18**
19 **20a** **20b**
20c: R = CHF_2
20d: R = Et
20e: R = *i*-Pr

[a]Reagents and conditions: (a) (1) $NaNO_2$, HCl aq, 0 °C, (2) methyl 4-methoxy-3-oxobutanoate, NaOAc, EtOH, 0 °C, 88%; (b) DMFDMA, reflux, 89%; (c) *N*,*O*-dimethylhydroxylamine hydrochloride, $AlMe_3$, DIPEA, CH_2Cl_2, 0 °C, 67%; (d) MeMgBr, THF, −78 °C, 79%; (e) DMFDMA, reflux, 89%; (f) phenylhydrazine, AcOH, reflux, 71%; (g) TMSCl, NaI, CH_3CN, reflux, 84%; (h) sodium chlorodifluoroacetate, K_2CO_3, DMF/water, 100 °C, 59%; (i) EtI or *i*-PrI, K_2CO_3, DMF, rt, 72−88%.

dx.doi.org/10.1021/jm5013648 | J. Med. Chem. XXXX, XXX, XXX−XXX

Scheme 4. Synthesis of Compounds 27a−h[a]

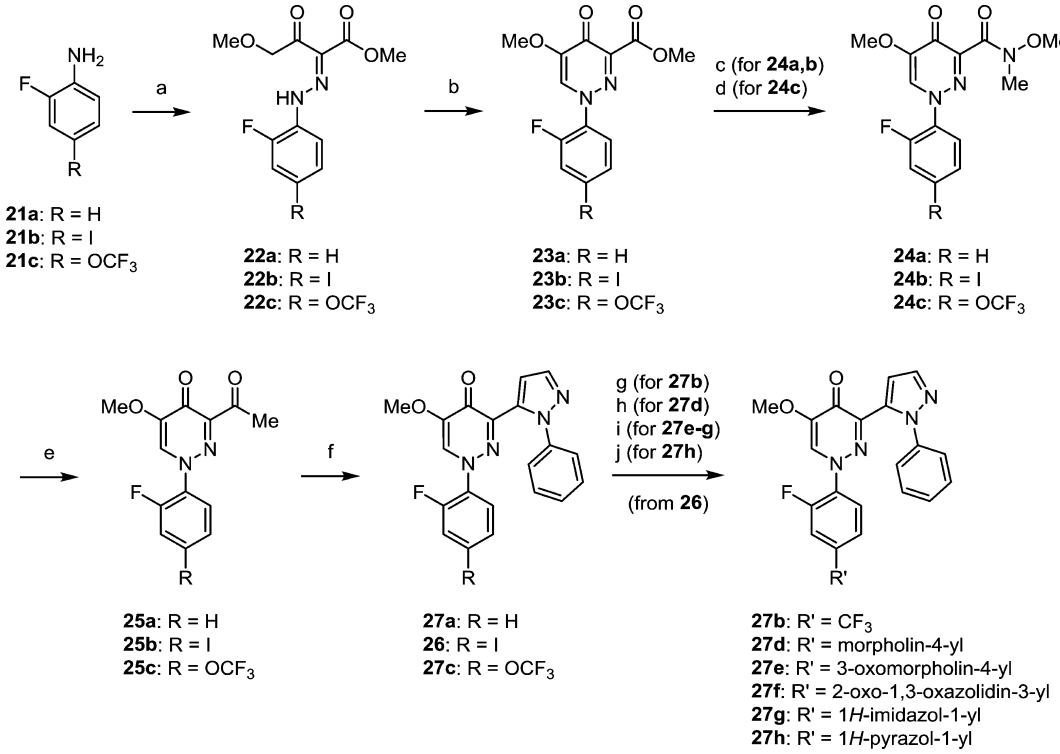

[a]Reagents and conditions: (a) (1) $NaNO_2$, HCl aq, 0 °C, (2) methyl 4-methoxy-3-oxobutanoate, NaOAc, EtOH, 0 °C, 58−94%; (b) DMFDMA, reflux, 59−90%; (c) *N,O*-dimethylhydroxylamine hydrochloride, $AlMe_3$, DIPEA, CH_2Cl_2, 0 °C, 65−77%; (d) (1) NaOH aq, MeOH, rt, (2) *N,O*-dimethylhydroxylamine hydrochloride, WSC·HCl, HOBt·H_2O, Et_3N, DMF, rt, 81%; (e) MeMgBr, THF, −78 °C, 23−85%; (f) (1) DMFDMA, reflux, (2) phenylhydrazine, AcOH, reflux, 45−66%; (g) methyl 2,2-fluoro-2-(fluorosulfonyl)acetate, CuI, HMPA, DMF, 90 °C, 33%; (h) morpholine, $Pd_2(dba)_3$, Xantphos, NaO*t*-Bu, 1,4-dioxane, 90 °C, 66%; (i) 3-morpholinone, 1,3-oxazolidin-2-one, or imidazole, CuI, *trans*-1,2-diaminocyclohexane, K_3PO_4, 1,4-dioxane, reflux, 8−71%; (j) pyrazole, Cu_2O, salicylaldoxime, Cs_2CO_3, CH_3CN, reflux, 44%.

Scheme 5. Synthesis of Compound 35[a]

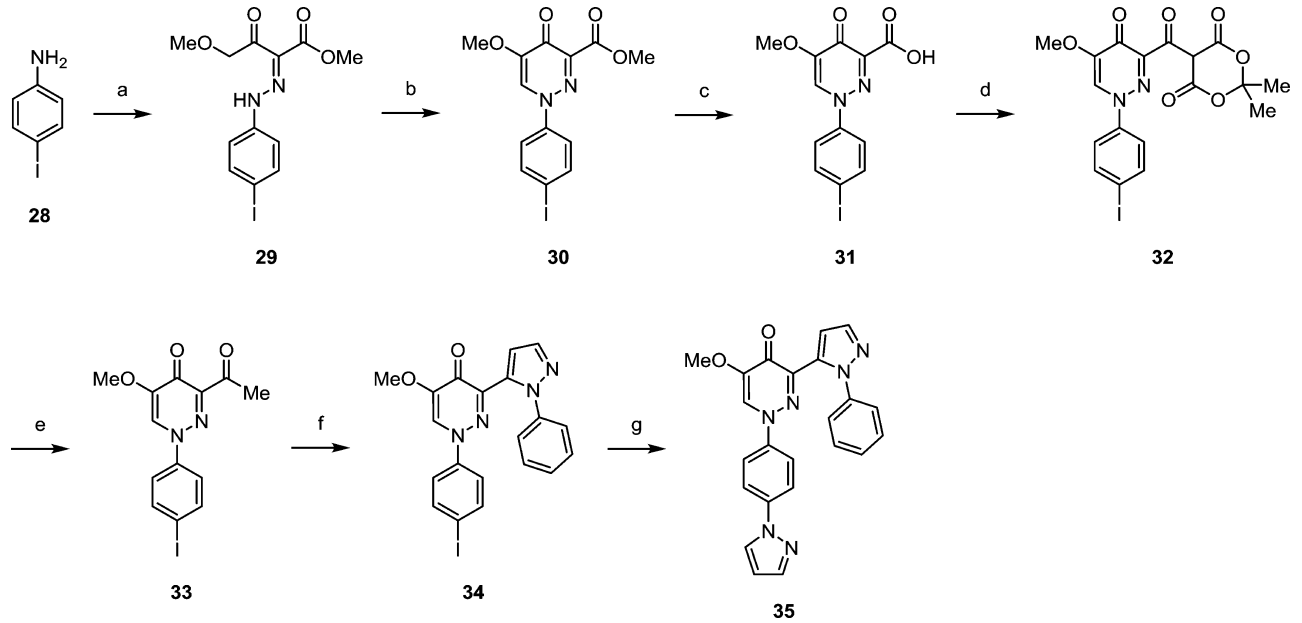

[a]Reagents and conditions: (a) (1) $NaNO_2$, HCl aq, 0 °C, (2) methyl 4-methoxy-3-oxobutanoate, NaOAc, EtOH, 0 °C, 78%; (b) DMFDMA, CH_3CN, reflux, 70%; (c) NaOH aq, MeOH, rt, 97%; (d) Meldrum's acid, WSC·HCl, DMAP, DMF, rt; (e) AcOH, water, reflux, 37% in 2 steps; (f) (1) DMFDMA, CH_3CN, reflux, (2) phenylhydrazine, TFA, EtOH, rt, 50%; (g) pyrazole, Cu_2O, salicylaldoxime, Cs_2CO_3, CH_3CN, reflux, 14%.

were carried out by Takeda Analytical Laboratories, and the results were within 0.4% of theoretical values.

Methyl 3-Oxo-2-{[3-(trifluoromethyl)phenyl]hydrazono}-butanoate (3). A solution of $NaNO_2$ (8.33 g, 121 mmol) in water

dx.doi.org/10.1021/jm5013648 | J. Med. Chem. XXXX, XXX, XXX−XXX

(20 mL) was added at 0 °C to a slurry of **2** (16.1 g, 100 mmol) in 6 M HCl aq (100 mL). The pale-yellow solution was poured into a suspension of methyl acetoacetate (11.6 g, 100 mmol) and NaOAc (150 g) in EtOH (170 mL) precooled at 0 °C. The resulting orange slurry was stirred for 10 min. The precipitate was collected by filtration and washed with water (500 mL). The crude material was dissolved in EtOAc (250 mL). The solution was dried over $MgSO_4$ and concentrated under reduced pressure to give **3** (a mixture of *E*/*Z*-isomers, 20.0 g, 69%) as a light-yellow solid. Major isomer: ^{1}H NMR ($CDCl_3$) δ 2.62 (3H, s), 3.90 (3H, s), 7.37−7.45 (1H, m), 7.46−7.54 (1H, m), 7.58 (1H, s), 7.67 (1H, s), 14.76 (1H, brs). Minor isomer: ^{1}H NMR ($CDCl_3$) δ 2.52 (3H, s), 3.93 (3H, s), 7.37−7.45 (1H, m), 7.46−7.54 (2H, m), 7.56 (1H, s), 12.81 (1H, brs).

*Methyl 4-Oxo-1-[3-(trifluoromethyl)phenyl]-1,4-dihydropyridazine-3-carboxylate (**4**).* A solution of **3** (15.2 g, 52.7 mmol) in DMFDMA (150 mL) was refluxed for 2 h. The mixture was cooled to rt and then on an ice−water bath. The precipitate was collected by filtration to give **4** (13.7 g, 87%) as a pale-yellow solid. ^{1}H NMR ($CDCl_3$) δ 4.00 (3H, s), 6.80 (1H, d, *J* = 8.1 Hz), 7.61−7.76 (2H, m), 7.76−7.91 (2H, m), 8.28 (1H, d, *J* =*J* = 8.1 Hz).

*4-Oxo-1-[3-(trifluoromethyl)phenyl]-1,4-dihydropyridazine-3-carboxamide (**5**).* A mixture of **4** (1.01 g, 3.38 mmol) and 7 M NH_3 in MeOH (12 mL) was heated at 100 °C for 5 min under microwave irradiation. The mixture was concentrated under reduced pressure, and the residue was recrystallized from EtOAc to give **5** (0.613 g, 64%) as a white solid. ^{1}H NMR ($CDCl_3$) δ 6.46 (1H, brs), 6.94 (1H, d, *J* = 7.8 Hz), 7.59−7.80 (2H, m), 7.84−8.01 (2H, m), 8.38 (1H, d, *J* = 7.8 Hz), 9.68 (1H, brs).

*N-[(Dimethylamino)methylene]-4-oxo-1-[3-(trifluoromethyl)-phenyl]-1,4-dihydropyridazine-3-carboxamide (**6**).* A slurry of **5** (540 mg, 1.91 mmol) in DMFDMA (10 mL) was heated at 130 °C for 15 min under microwave irradiation. The mixture was cooled on an ice−water bath, and the precipitate was collected by filtration and washed with hexane to give **6** (491 mg, 76%) as an off-white solid. ^{1}H NMR ($CDCl_3$) δ 3.16 (3H, s), 3.22 (3H, s), 6.72 (1H, d, *J* = 8.1 Hz), 7.57−7.71 (2H, m), 7.74−7.85 (1H, m), 7.89 (1H, s), 8.25 (1H, d, *J* = 8.1 Hz), 8.70 (1H, s).

*4-Oxo-1-[3-(trifluoromethyl)phenyl]-1,4-dihydropyridazine-3-carboxylic Acid (**7**).* To a suspension of **4** (10.0 g, 33.5 mmol) in MeOH (150 mL) was added 1 M NaOH aq (50 mL) at 0 °C. The mixture was stirred at rt for 30 min. To the suspension was added 1 M HCl aq (50 mL) at 0 °C, and the mixture was concentrated under reduced pressure. The residue was collected by filtration, washed with water, and dried under reduced pressure at 50 °C to give **7** (9.25 g, 97%) as a pale-yellow solid. ^{1}H NMR (DMSO-d_6) δ 7.02 (1H, d, *J* = 7.7 Hz), 7.81−7.96 (2H, m), 8.06−8.21 (2H, m), 9.16 (1H, d, *J* = 7.7 Hz).

*3-Amino-1-[3-(trifluoromethyl)phenyl]pyridazin-4(1H)-one (**8**).* A suspension of **7** (5.00 g, 17.6 mmol), DPPA (5.67 mL, 26.4 mmol), and Et_3N (3.65 mL, 26.4 mmol) in toluene (35 mL) was stirred at 100 °C for 2 h. After cooling to 0 °C, 8 M NaOH aq (22 mL) was added and the mixture was stirred at rt for 2 h. The mixture was diluted with brine and extracted with EtOAc. The organic layer was dried over Na_2SO_4 and concentrated under reduced pressure. The residue was suspended in EtOAc/IPE and filtered. The filtrate was concentrated under reduced pressure. The residue was purified by column chromatography (basic silica gel, 50:50 hexane/EtOAc to EtOAc) to give **8** (2.50 g, 56%) as a pale-yellow solid. ^{1}H NMR (DMSO-d_6) δ 6.17 (1H, d, *J* = 7.5 Hz), 6.52 (2H, brs), 7.67−7.81 (2H, m), 8.04 (1H, d, *J* = 7.5 Hz), 8.10 (1H, s), 8.75 (1H, d, *J* = 7.5 Hz).

*3-Bromo-1-[3-(trifluoromethyl)phenyl]pyridazin-4(1H)-one (**9**).* To a mixture of isoamyl nitrite (2.44 mL, 18.3 mmol) and $CuBr_2$ (1.89 g, 8.46 mmol) in DMF (18 mL) was added dropwise a solution of **8** (1.80 g, 7.05 mmol) in DMF (7.2 mL) at 0 °C. The mixture was stirred at 0 °C for 1 h and at 60 °C for 3 h. The mixture was diluted with brine and extracted with EtOAc. The organic layer was washed with brine, dried over $MgSO_4$, and concentrated under reduced pressure. The residue was purified by column chromatography (silica gel, 50:50 hexane/EtOAc to EtOAc) followed by trituration with hexane to give **9** (1.85 g, 82%) as a white solid. ^{1}H NMR (DMSO-d_6) δ 6.64 (1H, d, *J* = 7.7 Hz), 7.78−7.87 (2H, m), 8.01−8.07 (1H, m), 8.08 (1H, s), 9.00 (1H, d, *J* = 7.7 Hz).

*3-(2-Chloropyridin-3-yl)-1-[3-(trifluoromethyl)phenyl]pyridazin-4(1H)-one (**10**).* A mixture of **9** (300 mg, 0.94 mmol), (2-chloropyridin-3-yl)boronic acid (162 mg, 1.03 mmol), $Pd(PPh_3)_4$ (54.3 mg, 0.047 mmol), Na_2CO_3 (85.4 mg, 0.806 mmol), DME (3.6 mL), and water (1.1 mL) was stirred at 80 °C for 16 h and at 100 °C for 7 h under Ar atmosphere. The mixture was diluted with water and extracted with EtOAc. The organic layer was washed with saturated $NaHCO_3$ aq, dried over Na_2SO_4, and concentrated under reduced pressure. The residue was purified by column chromatography (basic silica gel, 80:20 hexane/EtOAc to EtOAc) followed by crystallization from EtOAc/hexane to give **10** (88.2 mg, 27%) as a white solid. ^{1}H NMR (DMSO-d_6) δ 6.74 (1H, d, *J* = 8.0 Hz), 7.59 (1H, dd, *J* = 7.6, 4.9 Hz), 7.79−7.87 (2H, m), 8.05−8.19 (3H, m), 8.54 (1H, dd, *J* = 4.9, 1.9 Hz), 9.05 (1H, d, *J* = 8.0 Hz).

*3-(1-Phenyl-1H-1,2,4-triazol-5-yl)-1-[3-(trifluoromethyl)phenyl]-pyridazin-4(1H)-one (**11a**).* A solution of **6** (119 mg, 0.35 mmol) and phenylhydrazine (0.070 mL, 0.71 mmol) in AcOH (5 mL) was heated at 120 °C for 10 min under microwave irradiation. The mixture was cooled to rt. The crude product was purified by column chromatography (silica gel, 85:15 EtOAc/MeOH) followed by recrystallization from EtOAc/hexane to give **11a** (126 mg, 94%) as an off-white solid; mp 174−176 °C. ^{1}H NMR ($CDCl_3$) δ 6.75 (1H, d, *J* = 8.1 Hz), 7.42−7.49 (5H, m), 7.50−7.54 (2H, m), 7.57−7.63 (1H, m), 7.66 (1H, d, *J* = 7.5 Hz), 8.23−8.25 (2H, m). LC-MS (ESI) *m*/*z* 384 $[M + H]^+$. Anal. Calcd for $C_{19}H_{12}F_3N_5O$: C, 59.53; H, 3.15; N, 18.27. Found: C, 59.50; H, 3.20; N, 18.11.

*3-(2-Phenyl-1H-imidazol-1-yl)-1-[3-(trifluoromethyl)phenyl]-pyridazin-4(1H)-one (**11b**).* A solution of **8** (200 mg, 0.783 mmol) and 40% glyoxal aq (0.0895 mL, 0.783 mmol) in MeOH (2 mL) was stirred at rt for 20 h. To the solution were added benzaldehyde (0.159 mL, 1.57 mmol) and NH_4Cl (84.0 mg, 1.57 mmol), and the mixture was refluxed for 90 min. To the mixture was added H_3PO_4 (0.106 mL, 1.98 mmol), and the mixture was refluxed for 24 h. The mixture was diluted with water and extracted with EtOAc. The organic layer was washed with saturated $NaHCO_3$ aq, dried over Na_2SO_4, and concentrated under reduced pressure. The residue was purified by column chromatography (silica gel, 50:50 hexane/EtOAc to EtOAc, and then basic silica gel, 50:50 hexane/EtOAc to EtOAc) followed by recrystallization from EtOAc/heptane to give **11b** (9.3 mg, 3%) as a white solid; mp 204−205 °C. ^{1}H NMR (DMSO-d_6) δ 6.82 (1H, d, *J* = 8.0 Hz), 7.20 (1H, d, *J* = 1.6 Hz), 7.33−7.41 (3H, m), 7.44−7.50 (2H, m), 7.62 (1H, s), 7.64−7.81 (4H, m), 9.06 (1H, d, *J* = 8.0 Hz). LC-MS (APCI) *m*/*z* 383 $[M + H]^+$. Anal. Calcd for $C_{20}H_{13}F_3N_4O$: C, 62.83; H, 3.43; N, 14.65. Found: C, 62.50; H, 3.64; N, 14.56.

*3-(2-Phenyl-3-furyl)-1-[3-(trifluoromethyl)phenyl]pyridazin-4(1H)-one (**11c**).* A mixture of **9** (300 mg, 0.94 mmol), (2-phenyl-3-furyl)boronic acid (265 mg, 1.41 mmol), $Pd(PPh_3)_4$ (54.3 mg, 0.047 mmol), Na_2CO_3 (299 mg, 2.82 mmol), DME (3.6 mL), and water (1.1 mL) was stirred at 80 °C for 4 h under Ar atmosphere. The mixture was diluted with water and extracted with EtOAc. The organic layer was washed with saturated $NaHCO_3$ aq, dried over Na_2SO_4, and concentrated under reduced pressure. The residue was purified by column chromatography (basic silica gel, 80:20 hexane/EtOAc to EtOAc) followed by recrystallization from EtOAc/heptane to give **11c** (23.9 mg, 7%) as a pale-yellow solid; mp 159−163 °C. ^{1}H NMR (DMSO-d_6) δ 6.63 (1H, d, *J* = 8.0 Hz), 6.99 (1H, d, *J* = 1.9 Hz), 7.32−7.43 (3H, m), 7.54−7.60 (2H, m), 7.69−7.76 (2H, m), 7.78−7.82 (1H, m), 7.85 (1H, d, *J* = 1.9 Hz), 7.85−7.92 (1H, m), 8.96 (1H, d, *J* = 8.0 Hz). LC-MS (APCI) *m*/*z* 383 $[M + H]^+$. Anal. Calcd for $C_{21}H_{13}F_3N_2O_2 \cdot 0.3H_2O$: C, 65.05; H, 3.54; N, 7.22. Found: C, 65.20; H, 3.63; N, 7.29.

*3-(2-Phenylpyridin-3-yl)-1-[3-(trifluoromethyl)phenyl]pyridazin-4(1H)-one (**11d**).* A mixture of **10** (74.5 mg, 0.212 mmol), phenylboronic acid (31.0 mg, 0.254 mmol), $Pd(PPh_3)_4$ (12.2 mg, 0.0106 mmol), Na_2CO_3 (33.7 mg, 0.318 mmol), DME (2.1 mL), and water (0.7 mL) was stirred at 80 °C for 40 h under Ar atmosphere. The mixture was diluted with saturated $NaHCO_3$ aq and extracted with EtOAc. The organic layer was dried over Na_2SO_4 and concentrated under reduced pressure. The residue was purified by preparative HPLC followed by recrystallization from EtOAc/heptane to give **11d** (29.7 mg, 36%) as a white solid; mp 192−194 °C. ^{1}H NMR (DMSO-d_6) δ 6.58 (1H, d, *J* = 8.0 Hz), 7.29−7.43 (5H, m), 7.51 (1H, dd, *J* = 7.8, 4.8 Hz), 7.55 (1H, s), 7.68−7.78 (3H, m), 8.06 (1H, dd, *J* = 7.8, 1.8 Hz), 8.75

dx.doi.org/10.1021/jm5013648 | *J. Med. Chem.* XXXX, XXX, XXX−XXX

(1H, dd, J = 4.7, 1.6 Hz), 8.91 (1H, d, J = 8.0 Hz). LC-MS (APCI) m/z 394 $[M + H]^+$. Anal. Calcd for $C_{22}H_{14}F_3N_3O{\cdot}0.4H_2O$: C, 66.00; H, 3.72; N, 10.49. Found: C, 66.06; H, 3.69; N, 10.47.

*3-{[2-(Trifluoromethyl)phenyl]hydrazono}pentane-2,4-dione (**13a**).* A solution of $NaNO_2$ (0.563 g, 8.16 mmol) in water (4 mL) was added dropwise at 0 °C to a mixture of **12a** (1.09 g, 6.80 mmol), concentrated HCl aq (5 mL), and water (5 mL). After stirring at 0 °C for 1 h, the resulting aqueous solution was added dropwise to a mixture of acetylacetone (0.748 g, 7.48 mmol), NaOAc (1.67 g, 20.4 mmol), EtOH (10 mL), and water (6 mL). The mixture was stirred at rt overnight. The precipitate was collected by filtration, washed successively with water, EtOH/water (1/1), and hexane, and dried to give **13a** (0.634 g, 33%) as an orange solid. ^1H NMR ($CDCl_3$) δ 2.52 (3H, s), 2.63 (3H, s), 7.45–7.44 (1H, m), 7.58–7.51 (2H, m), 7.66 (1H, s), 14.68 (1H, s).

*3-[(2-Methylphenyl)hydrazono]pentane-2,4-dione (**13b**).* Compound **13b** was obtained (49%) as an orange solid in a manner similar to that described for the synthesis of **13a**. LC-MS (ESI) m/z 219 $[M + H]^+$.

*3-[(2-Chlorophenyl)hydrazono]pentane-2,4-dione (**13c**).* Compound **13c** was obtained (46%) as an orange solid in a manner similar to that described for the synthesis of **13a**. ^1H NMR ($CDCl_3$) δ 2.52 (3H, s), 2.64 (3H, s), 7.11–7.15 (1H, m), 7.34–7.37 (1H, m), 7.42 (1H, dd, J = 8.0, 1.2 Hz), 7.81 (1H, dd, J = 8.0, 1.2 Hz), 14.88 (1H, s).

*3-[(2-Fluorophenyl)hydrazono]pentane-2,4-dione (**13d**).* Compound **13d** was obtained (64%) as an orange solid in a manner similar to that described for the synthesis of **13a**. ^1H NMR ($CDCl_3$) δ 2.51 (3H, s), 2.62 (3H, s), 7.14–7.24 (3H, m), 7.77 (1H, d, J = 8.0 Hz), 14.71 (1H, s).

*3-(Phenylhydrazono)pentane-2,4-dione (**13e**).* Compound **13e** was obtained (67%) as an orange solid in a manner similar to that described for the synthesis of **13a**. ^1H NMR ($CDCl_3$) δ 2.50 (3H, s), 2.61 (3H, s), 7.21 (1H, dd, J = 8.0, 4.4 Hz), 7.41 (4H, d, J = 4.4 Hz), 14.74 (1H, s).

*3-(1-Phenyl-1H-pyrazol-5-yl)-1-[2-(trifluoromethyl)phenyl]-pyridazin-4(1H)-one (**14a**).* A solution of **13a** (634 mg, 2.33 mmol) in DMFDMA (10 mL) was refluxed for 4 h and then concentrated under reduced pressure. A solution of the residue and phenylhydrazine (377 mg, 3.50 mmol) in MeOH (20 mL) was refluxed for 4 h and then concentrated under reduced pressure. The residue was dissolved in CH_2Cl_2, washed with 1 M HCl aq and brine, dried over Na_2SO_4, and concentrated under reduced pressure. The residue was subjected to preparative HPLC to give **14a** (105 mg, 12%). An analytical sample was obtained as a white solid by purification by column chromatography (basic silica gel, EtOAc) and subsequent crystallization from EtOAc/hexane; mp 154–156 °C. ^1H NMR ($CDCl_3$) δ 6.58 (1H, d, J = 7.9 Hz), 6.94–7.00 (1H, m), 7.14 (1H, d, J = 2.1 Hz), 7.23–7.37 (5H, m), 7.54–7.63 (2H, m), 7.73–7.81 (3H, m). LC-MS (ESI) m/z 383 $[M + H]^+$. Anal. Calcd for $C_{20}H_{13}F_3N_4O$: C, 62.83; H, 3.43; N, 14.65. Found: C, 62.98; H, 3.53; N, 14.63.

*1-(2-Methylphenyl)-3-(1-phenyl-1H-pyrazol-5-yl)pyridazin-4(1H)-one (**14b**).* Compound **14b** was prepared (12%) in a manner similar to that described for the synthesis of **14a**. An analytical sample was obtained as a white solid by purification by column chromatography (basic silica gel, EtOAc) and subsequent crystallization from EtOAc/hexane; mp 115–117 °C. ^1H NMR ($CDCl_3$) δ 1.99 (3H, s), 6.64 (1H, d, J = 7.7 Hz), 6.81 (1H, dd, J = 7.7, 1.1 Hz), 7.14 (1H, d, J = 1.9 Hz), 7.16–7.24 (2H, m), 7.29–7.38 (6H, m), 7.77 (1H, d, J = 1.9 Hz), 7.79 (1H, d, J = 7.7 Hz). LC-MS (ESI) m/z 329 $[M + H]^+$. Anal. Calcd for $C_{20}H_{16}N_4O$: C, 73.15; H, 4.91; N, 17.06. Found: C, 73.08; H, 4.93; N, 17.02.

*1-(2-Chlorophenyl)-3-(1-phenyl-1H-pyrazol-5-yl)pyridazin-4(1H)-one (**14c**).* Compound **14c** was prepared (8%) in a manner similar to that described for the synthesis of **14a**. An analytical sample was obtained as an off-white solid by purification by column chromatography (basic silica gel, EtOAc) and subsequent crystallization from EtOAc/hexane; mp 147–149 °C. ^1H NMR ($CDCl_3$) δ 6.63 (1H, d, J = 7.7 Hz), 6.68 (1H, dd, J = 7.9, 1.5 Hz), 7.18–7.24 (2H, m), 7.31–7.39 (6H, m), 7.46 (1H, dd, J = 7.9, 1.5 Hz), 7.77 (1H, d, J = 1.9 Hz), 7.90 (1H, d, J = 7.9 Hz). LC-MS (ESI) m/z 349 $[M + H]^+$. Anal. Calcd for $C_{19}H_{13}ClN_4O$: C, 65.43; H, 3.76; N, 16.06. Found: C, 65.41; H, 3.78; N, 15.97.

*1-(2-Fluorophenyl)-3-(1-phenyl-1H-pyrazol-5-yl)pyridazin-4(1H)-one (**14d**).* Compound **14d** was prepared (31%) in a manner similar to that described for the synthesis of **14a**. An analytical sample was obtained as a white solid by purification by column chromatography (basic silica gel, EtOAc) and subsequent crystallization from EtOAc/hexane; mp 129–131 °C. ^1H NMR ($CDCl_3$) δ 6.44 (1H, td, J = 8.0, 1.7 Hz), 6.65 (1H, d, J = 7.9 Hz), 6.98–7.04 (1H, m), 7.17 (1H, ddd, J = 11.3, 8.4, 1.3 Hz), 7.27–7.46 (7H, m), 7.79 (1H, d, J = 1.9 Hz), 8.02 (1H, dd, J = 7.9, 2.6 Hz). LC-MS (ESI) m/z 333 $[M + H]^+$. Anal. Calcd for $C_{19}H_{13}FN_4O$: C, 68.67; H, 3.93; N, 16.85. Found: C, 68.68; H, 3.98; N, 16.81.

*1-Phenyl-3-(1-phenyl-1H-pyrazol-5-yl)pyridazin-4(1H)-one (**14e**).* Compound **14e** was prepared (7%) in a manner similar to that described for the synthesis of **14a**. An analytical sample was obtained as a white solid by purification by column chromatography (basic silica gel, EtOAc) and subsequent recrystallization from EtOAc/hexane; mp 188–190 °C. ^1H NMR ($CDCl_3$) δ 6.71 (1H, d, J = 7.9 Hz), 6.79–6.85 (2H, m), 7.27–7.32 (3H, m), 7.37–7.48 (6H, m), 7.80 (1H, d, J = 1.9 Hz), 8.17 (1H, d, J = 7.9 Hz). LC-MS (ESI) m/z 315 $[M + H]^+$. Anal. Calcd for $C_{19}H_{14}N_4O$: C, 72.60; H, 4.49; N, 17.82. Found: C, 72.52; H, 4.53; N, 17.74

*Methyl 4-Methoxy-3-oxo-2-{[3-(trifluoromethyl)phenyl]-hydrazono}butanoate (**15**).* A solution of $NaNO_2$ (4.14 g, 60 mmol) in water (15 mL) was added dropwise at 0 °C to a mixture of **2** (6.24 mL, 50 mmol) and 6 M HCl aq (50 mL, 300 mmol). After stirring for 15 min, the resulting aqueous solution was added to a suspension of methyl 4-methoxy-3-oxobutanoate (7.31 mL, 50 mmol) and NaOAc (24.6 g, 300 mmol) in EtOH (80 mL) precooled at 0 °C. The precipitate was collected by filtration, washed with water, and dissolved in EtOAc. The organic solution was washed with water and brine, dried over Na_2SO_4, and concentrated under reduced pressure. The residue was crystallized from EtOAc/hexane to give **15** (a mixture of E/Z-isomers, 14.0 g, 88%) as a pale-yellow solid. ^1H NMR ($CDCl_3$) δ 3.51 (3H × 0.36, s), 3.52 (3H × 0.64, s), 3.90 (3H × 0.36, s), 3.94 (3H × 0.64, s), 4.68 (2H × 0.64, s), 4.70 (2H × 0.36, s), 7.41–7.59 (3H + 1H × 0.64, m), 7.71 (1H × 0.36, s), 13.00 (1H × 0.64, s), 14.87 (1H × 0.36, s).

*Methyl 5-Methoxy-4-oxo-1-[3-(trifluoromethyl)phenyl]-1,4-dihydropyridazine-3-carboxylate (**16**).* A solution of **15** (14.0 g, 44 mmol) in DMFDMA (100 mL) was refluxed for 4 h. After cooling to rt, the precipitate was collected by filtration and washed with hexane/EtOAc (3/1) to give **16** (12.9 g, 89%) as an off-white solid. ^1H NMR ($CDCl_3$) δ 3.98 (3H, s), 3.99 (3H, s), 7.66–7.74 (2H, m), 7.83–7.89 (2H, m), 7.95 (1H, s).

*N,5-Dimethoxy-N-methyl-4-oxo-1-[3-(trifluoromethyl)phenyl]-1,4-dihydropyridazine-3-carboxamide (**17**).* To a solution of *N,O*-dimethylhydroxylamine hydrochloride (2.63 g, 27 mmol) and DIPEA (4.70 mL, 27 mmol) in CH_2Cl_2 (30 mL) was added $AlMe_3$ (1.8 M solution in toluene, 15 mL, 27 mmol) dropwise at 0 °C under Ar atmosphere. After stirring for 1 h, a solution of **16** (2.95 g, 9 mmol) in CH_2Cl_2 (30 mL) was added dropwise and the mixture was stirred at 0 °C for 1 h. The mixture was poured into ice–water and extracted with EtOAc. The organic layer was washed with brine, dried over $MgSO_4$, and concentrated under reduced pressure. The residue was purified by column chromatography (basic silica gel, EtOAc) followed by recrystallization from EtOAc/hexane to give **17** (2.15 g, 67%) as an off-white solid. ^1H NMR ($CDCl_3$) δ 3.41 (3H, s), 3.71 (3H, s), 3.98 (3H, s), 7.63–7.71 (2H, m), 7.80–7.86 (1H, m), 7.88 (1H, s), 7.98 (1H, s).

*3-Acetyl-5-methoxy-1-[3-(trifluoromethyl)phenyl]pyridazin-4(1H)-one (**18**).* To a solution of **17** (2.09 g, 5.85 mmol) in THF (50 mL) was added MeMgBr (3 M solution in diethyl ether, 4 mL, 12 mmol) dropwise at −78 °C. After stirring for 1 h, the mixture was quenched with saturated NH_4Cl aq and extracted with EtOAc three times. The combined organic layers were washed with brine, dried over $MgSO_4$, and concentrated under reduced pressure. The residue was purified by column chromatography (silica gel, EtOAc to 91:9 EtOAc/MeOH) followed by recrystallization from EtOAc/hexane to give **18** (1.44 g, 79%) as an off-white solid. ^1H NMR ($CDCl_3$) δ 2.71 (3H, s), 3.98 (3H, s), 7.68–7.76 (2H, m), 7.83–7.88 (2H, m), 7.94 (1H, s).

*3-[3-(Dimethylamino)prop-2-enoyl]-5-methoxy-1-[3-(trifluoromethyl)phenyl]pyridazin-4(1H)-one (**19**).* A solution of **18**

dx.doi.org/10.1021/jm5013648 | J. Med. Chem. XXXX, XXX, XXX–XXX

(1.39 g, 4.45 mmol) in DMFDMA (15 mL) was refluxed for 3 h. After cooling to rt, the mixture was concentrated under reduced pressure, and the residue was dissolved in EtOAc. The organic solution was washed with half-saturated brine, and the aqueous solution was extracted with EtOAc four times. The combined organic layers were dried over $MgSO_4$ and concentrated under reduced pressure. The residue was recrystallized from EtOAc to give **19** (1.46 g, 89%) as an orange solid. ^{1}H NMR ($CDCl_3$) δ 2.91 (3H, s), 3.14 (3H, s), 3.96 (3H, s), 5.80 (1H, d, J = 13.2 Hz), 7.61−7.68 (2H, m), 7.80 (1H, brs), 7.84−7.90 (2H, m), 7.96 (1H, s).

*5-Methoxy-3-(1-phenyl-1H-pyrazol-5-yl)-1-[3-(trifluoromethyl)-phenyl]pyridazin-4(1H)-one (**20a**).* A solution of **19** (3.41 g, 9.29 mmol) and phenylhydrazine (1.83 mL, 18.6 mmol) in AcOH (25 mL) was refluxed for 2 h. After cooling to rt, the mixture was concentrated under reduced pressure. The residue was diluted with EtOAc, washed successively with 1 M HCl aq, 1 M NaOH aq, and brine, dried over $MgSO_4$, and concentrated under reduced pressure. The residue was purified by column chromatography (silica gel, EtOAc) followed by crystallization from EtOAc/hexane to give **20a** (2.70 g, 71%) as a white solid; mp 139−141 °C. ^{1}H NMR ($CDCl_3$) δ 3.98 (3H, s), 7.05 (1H, dd, J = 7.9, 1.9 Hz), 7.19 (1H, s), 7.34−7.47 (7H, m), 7.56 (1H, d, J = 7.9 Hz), 7.80 (1H, d, J = 1.9 Hz), 7.92 (1H, s). LC-MS (ESI) m/z 413 $[M + H]^+$. Anal. Calcd for $C_{21}H_{15}F_3N_4O_2$: C, 61.17; H, 3.67; N, 13.59. Found: C, 61.15; H, 3.65; N, 13.57.

*5-Hydroxy-3-(1-phenyl-1H-pyrazol-5-yl)-1-[3-(trifluoromethyl)-phenyl]pyridazin-4(1H)-one (**20b**).* TMSCl (3.17 mL, 25 mmol) was added at rt to a solution of NaI (3.75 g, 25 mmol) in CH_3CN (150 mL). After stirring for 30 min, **20a** (2.06 g, 5 mmol) was added, and the mixture was stirred at rt for 30 min and then refluxed for 1 h. The mixture was poured into water and extracted with EtOAc. The organic layer was washed with brine, dried over $MgSO_4$, and concentrated under reduced pressure. The residue was washed with EtOAc/hexane (1/1) and recrystallized from MeOH/water to give **20b** (1.68 g, 84%) as a white solid; mp 246−248 °C. ^{1}H NMR (DMSO-d_6) δ 7.17 (1H, d, J = 1.9 Hz), 7.33−7.46 (5H, m), 7.53−7.64 (3H, m), 7.71 (1H, d, J = 7.5 Hz), 7.83 (1H, d, J = 1.9 Hz), 8.83 (1H, s). Anal. Calcd for $C_{20}H_{13}F_3N_4O_2$: C, 60.30; H, 3.29; N, 14.07. Found: C, 60.09; H, 3.33; N, 14.02.

*5-(Difluoromethoxy)-3-(1-phenyl-1H-pyrazol-5-yl)-1-[3-(trifluoromethyl)phenyl]pyridazin-4(1H)-one (**20c**).* A mixture of **20b** (398 mg, 1.0 mmol), sodium chlorodifluoroacetate (305 mg, 2.0 mmol), K_2CO_3 (207 mg, 1.5 mmol), DMF (2 mL), and water (0.4 mL) was stirred at 100 °C for 6 h. The mixture was poured into water and extracted with EtOAc. The organic layer was washed with brine, dried over $MgSO_4$, and concentrated under reduced pressure. The residue was purified by column chromatography (basic silica gel, 75:25 hexane/EtOAc) followed by crystallization from EtOAc/hexane to give **20c** (267 mg, 59%) as a white solid; mp 132−134 °C. ^{1}H NMR ($CDCl_3$) δ 7.06 (1H, dd, J = 8.3, 2.3 Hz), 7.16−7.66 (10H, m), 7.82 (1H, d, J = 1.9 Hz), 8.33 (1H, s). LC-MS (ESI) m/z 449 $[M + H]^+$. Anal. Calcd for $C_{21}H_{13}F_5N_4O_2$: C, 56.26; H, 2.92; N, 12.50. Found: C, 55.98; H, 2.82; N, 12.43.

*5-Ethoxy-3-(1-phenyl-1H-pyrazol-5-yl)-1-[3-(trifluoromethyl)-phenyl]pyridazin-4(1H)-one (**20d**).* A suspension of **20b** (100 mg, 0.25 mmol), iodoethane (0.040 mL, 0.50 mmol), and K_2CO_3 (104 mg, 0.75 mmol) in DMF (1 mL) was stirred at rt for 24 h. The mixture was poured into water and extracted with EtOAc. The organic layer was washed with brine, dried over $MgSO_4$, and concentrated under reduced pressure. The residue was purified by column chromatography (basic silica gel, 50:50 hexane/EtOAc) to give **20d** (94.1 mg, 88%) as an off-white amorphous solid. ^{1}H NMR ($CDCl_3$) δ 1.52 (3H, t, J = 6.8 Hz), 4.21 (2H, q, J = 6.8 Hz), 7.03 (1H, dd, J = 7.9, 1.9 Hz), 7.18 (1H, s), 7.33−7.46 (7H, m), 7.55 (1H, d, J = 7.9 Hz), 7.80 (1H, d, J = 1.9 Hz), 7.94 (1H, s). LC-MS (ESI) m/z 413 $[M + H]^+$. Anal. Calcd for $C_{22}H_{17}F_3N_4O_2$: C, 61.97; H, 4.02; N, 13.14. Found: C, 61.82; H, 4.15; N, 13.17.

*5-Isopropoxy-3-(1-phenyl-1H-pyrazol-5-yl)-1-[3-(trifluoromethyl)-phenyl]pyridazin-4(1H)-one (**20e**).* Compound **20e** was obtained (72%) as a white solid in a manner similar to that described for the synthesis of **20d**; mp 137−139 °C. ^{1}H NMR ($CDCl_3$) δ 1.38 (6H, d, J = 6.4 Hz), 4.96−5.09 (1H, m), 7.05 (1H, dd, J = 7.9, 1.9 Hz), 7.18 (1H, s), 7.33−7.46 (7H, m), 7.55 (1H, d, J = 7.9 Hz), 7.80 (1H, d, J = 1.9 Hz), 8.01 (1H, s). LC-MS (ESI) m/z 441 $[M + H]^+$. Anal. Calcd for $C_{23}H_{19}F_3N_4O_2$: C, 62.72; H, 4.35; N, 12.72. Found: C, 62.74; H, 4.40; N, 12.81.

*Methyl 2-[(2-Fluorophenyl)hydrazono]-4-methoxy-3-oxobutanoate (**22a**).* Compound **22a** was obtained (94%) as a pale-yellow solid in a manner similar to that described for the synthesis of **15**. ^{1}H NMR ($CDCl_3$) δ 3.51 (3H, s), 3.94 (3H, s), 4.68 (2H, s), 7.08−7.25 (3H, m), 7.63 (1H, td, J = 7.9, 1.5 Hz), 13.06 (1H, brs).

*Methyl 2-[(2-Fluoro-4-iodophenyl)hydrazono]-4-methoxy-3-oxobutanoate (**22b**).* Compound **22b** was obtained (80%) as a yellow solid in a manner similar to that described for the synthesis of **15**. ^{1}H NMR ($CDCl_3$) δ 3.50 (3H, s), 3.93 (3H, s), 4.64 (2H, s), 7.35 (1H, t, J = 8.5 Hz), 7.49−7.55 (2H, m), 12.97 (1H, brs).

*Methyl 2-{[2-Fluoro-4-(trifluoromethoxy)phenyl]hydrazono}-4-methoxy-3-oxobutanoate (**22c**).* Compound **22c** was obtained (58%) as a yellow solid in a manner similar to that described for the synthesis of **15**. ^{1}H NMR ($CDCl_3$) δ 3.51 (3H, s), 3.94 (3H, s), 4.65 (2H, s), 7.06−7.14 (2H, m), 7.59−7.68 (1H, m), 12.98 (1H, brs).

*Methyl 1-(2-Fluorophenyl)-5-methoxy-4-oxo-1,4-dihydropyridazine-3-carboxylate (**23a**).* Compound **23a** was obtained (90%) as an off-white solid in a manner similar to that described for the synthesis of **16**. ^{1}H NMR ($CDCl_3$) δ 3.91 (3H, s), 3.97 (3H, s), 7.29−7.36 (2H, m), 7.44−7.51 (1H, m), 7.65 (1H, td, J = 7.9, 1.9 Hz), 7.77 (1H, d, J = 2.3 Hz).

*Methyl 1-(2-Fluoro-4-iodophenyl)-5-methoxy-4-oxo-1,4-dihydropyridazine-3-carboxylate (**23b**).* A solution of **22b** (6.27 g, 15.9 mmol) in DMFDMA (60 mL) was refluxed for 3 h. The mixture was poured into water and extracted with EtOAc. The organic layer was washed with water and brine, dried over $MgSO_4$, and concentrated under reduced pressure. The residue was purified by column chromatography (silica gel, EtOAc) followed by recrystallization from MeOH to give **23b** (3.77 g, 59%) as an off-white solid. ^{1}H NMR ($CDCl_3$) δ 3.90 (3H, s), 3.97 (3H, s), 7.36−7.41 (1H, m), 7.64−7.70 (2H, m), 7.73 (1H, d, J = 2.6 Hz).

*Methyl 1-[2-Fluoro-4-(trifluoromethoxy)phenyl]-5-methoxy-4-oxo-1,4-dihydropyridazine-3-carboxylate (**23c**).* Compound **23c** was obtained (67%) as an off-white solid in a manner similar to that described for the synthesis of **23b**. ^{1}H NMR ($CDCl_3$) δ 3.91 (3H, s), 3.97 (3H, s), 7.18−7.25 (2H, m), 7.69−7.75 (2H, m).

*1-(2-Fluorophenyl)-N,5-dimethoxy-N-methyl-4-oxo-1,4-dihydropyridazine-3-carboxamide (**24a**).* Compound **24a** was obtained (65%) as a white solid in a manner similar to that described for the synthesis of **17**. ^{1}H NMR ($CDCl_3$) δ 3.39 (3H, s), 3.71 (3H, s), 3.91 (3H, s), 7.25−7.33 (2H, m), 7.41−7.48 (1H, m), 7.65 (1H, td, J = 7.9, 1.9 Hz), 7.81 (1H, d, J = 2.3 Hz).

*1-(2-Fluoro-4-iodophenyl)-N,5-dimethoxy-N-methyl-4-oxo-1,4-dihydropyridazine-3-carboxamide (**24b**).* Compound **24b** was obtained (77%) as a white amorphous solid in a manner similar to that described for the synthesis of **17**. ^{1}H NMR ($CDCl_3$) δ 3.39 (3H, s), 3.70 (3H, s), 3.90 (3H, s), 7.39 (1H, t, J = 8.1 Hz), 7.63−7.67 (2H, m), 7.77 (1H, d, J = 2.3 Hz).

*1-[2-Fluoro-4-(trifluoromethoxy)phenyl]-N,5-dimethoxy-N-methyl-4-oxo-1,4-dihydropyridazine-3-carboxamide (**24c**).* A solution of **23c** (362 mg, 1.0 mmol) and 2 M NaOH aq (0.75 mL, 1.5 mmol) in MeOH (3 mL) was stirred at rt for 1 h. The mixture was poured into water, neutralized with 2 M HCl aq, and extracted with EtOAc. The organic layer was washed with brine, dried over $MgSO_4$, and concentrated under reduced pressure.

A suspension of the residue, *N,O*-dimethylhydroxylamine hydrochloride (107 mg, 1.1 mmol), WSC·HCl (230 mg, 1.2 mmol), HOBt·H_2O (184 mg, 1.2 mmol), and Et_3N (0.153 mL, 1.1 mmol) in DMF (3 mL) was stirred at rt for 4 h. The mixture was poured into water and extracted with EtOAc. The organic layer was washed with water and brine, dried over $MgSO_4$, and concentrated under reduced pressure. The residue was purified by column chromatography (basic silica gel, 50:50 hexane/EtOAc) to give **24c** (317 mg, 81%) as an off-white amorphous solid. ^{1}H NMR ($CDCl_3$) δ 3.39 (3H, s), 3.71 (3H, s), 3.91 (3H, s), 7.17−7.22 (2H, m), 7.73 (1H, t, J = 8.6 Hz), 7.77 (1H, d, J = 2.3 Hz).

*3-Acetyl-1-(2-fluorophenyl)-5-methoxypyridazin-4(1H)-one (**25a**).* Compound **25a** was obtained (85%) as a pale-yellow solid in a manner similar to that described for the synthesis of **18**. ^{1}H NMR

dx.doi.org/10.1021/jm5013648 | J. Med. Chem. XXXX, XXX, XXX−XXX

($CDCl_3$) δ 2.69 (3H, s), 3.91 (3H, s), 7.27−7.38 (2H, m), 7.45−7.53 (1H, m), 7.65 (1H, td, J = 7.9, 1.5 Hz), 7.77 (1H, d, J = 2.3 Hz).

*3-Acetyl-1-(2-fluoro-4-iodophenyl)-5-methoxypyridazin-4(1H)-one (**25b**).* Compound **25b** was obtained (23%) as a pale-yellow solid in a manner similar to that described for the synthesis of **18**. ^{1}H NMR ($CDCl_3$) δ 2.67 (3H, s), 3.90 (3H, s), 7.36−7.41 (1H, m), 7.66−7.71 (2H, m), 7.73 (1H, d, J = 2.6 Hz).

*3-Acetyl-1-[2-fluoro-4-(trifluoromethoxy)phenyl]-5-methoxypyridazin-4(1H)-one (**25c**).* Compound **25c** was obtained (79%) as a pale-yellow solid in a manner similar to that described for the synthesis of **18**. ^{1}H NMR ($CDCl_3$) δ 2.68 (3H, s), 3.91 (3H, s), 7.19−7.25 (2H, m), 7.69−7.75 (2H, m).

*1-(2-Fluoro-4-iodophenyl)-5-methoxy-3-(1-phenyl-1H-pyrazol-5-yl)-pyridazin-4(1H)-one (**26**).* A solution of **25b** (2.02 g, 5.2 mmol) in DMFDMA (30 mL) was refluxed for 6 h. After cooling to room temperature, the reaction mixture was concentrated under reduced pressure.

A solution of the residue and phenylhydrazine (1.54 mL, 15.6 mmol) in AcOH (20 mL) was refluxed for 2 h. After cooling to room temperature, the reaction mixture was concentrated under reduced pressure. The residue was diluted with EtOAc, washed successively with 1 M HCl aq, 1 M NaOH aq, and brine, dried over $MgSO_4$, and concentrated under reduced pressure. The residue was purified by column chromatography (silica gel, EtOAc) followed by recrystallization from EtOAc to give **26** (1.14 g, 45%) as a pale-yellow solid. ^{1}H NMR ($CDCl_3$) δ 3.90 (3H, s), 6.04 (1H, t, J = 8.5 Hz), 7.30−7.47 (7H, m), 7.54 (1H, dd, J = 10.6, 1.9 Hz), 7.76 (1H, d, J = 2.3 Hz), 7.78 (1H, d, J = 2.3 Hz).

*1-(2-Fluorophenyl)-5-methoxy-3-(1-phenyl-1H-pyrazol-5-yl)-pyridazin-4(1H)-one (**27a**).* Compound **27a** was obtained (59%) as a white solid in a manner similar to that described for the synthesis of **26**; mp 163−165 °C. ^{1}H NMR ($CDCl_3$) δ 3.90 (3H, s), 6.43 (1H, td, J = 7.9, 1.5 Hz), 6.98−7.04 (1H, m), 7.18 (1H, ddd, J = 11.3, 8.3, 1.1 Hz), 7.28−7.46 (7H, m), 7.78 (1H, d, J = 1.9 Hz), 7.81 (1H, d, J = 2.3 Hz). LC-MS (ESI) m/z 363 $[M + H]^+$. Anal. Calcd for $C_{20}H_{15}FN_4O_2$: C, 66.29; H, 4.17; N, 15.46. Found: C, 66.09; H, 4.22; N, 15.42.

*1-[2-Fluoro-4-(trifluoromethyl)phenyl]-5-methoxy-3-(1-phenyl-1H-pyrazol-5-yl)pyridazin-4(1H)-one (**27b**).* A suspension of **26** (244 mg, 0.5 mmol), methyl 2,2-fluoro-2-(fluorosulfonyl)acetate (0.318 mL, 2.5 mmol), CuI (114 mg, 0.6 mmol), and HMPA (0.435 mL, 2.5 mmol) in DMF (2.5 mL) was stirred at 90 °C for 24 h under Ar atmosphere. The mixture was poured into water and extracted with EtOAc. The organic layer was washed with brine, dried over $MgSO_4$, and concentrated under reduced pressure. The residue was purified by column chromatography (basic silica gel, 50:50 hexane/EtOAc) followed by recrystallization from EtOAc/hexane to give **27b** (71.7 mg, 33%) as an off-white solid; mp 169−171 °C. ^{1}H NMR ($CDCl_3$) δ 3.92 (3H, s), 6.42−6.47 (1H, m), 7.22−7.26 (1H, m), 7.37−7.49 (7H, m), 7.80 (1H, d, J = 1.9 Hz), 7.84 (1H, d, J = 2.3 Hz). LC-MS (ESI) m/z 431 $[M + H]^+$. Anal. Calcd for $C_{21}H_{14}F_4N_4O_2$: C, 58.61; H, 3.28; N, 13.02. Found: C, 58.50; H, 3.36; N, 12.93.

*1-[2-Fluoro-4-(trifluoromethoxy)phenyl]-5-methoxy-3-(1-phenyl-1H-pyrazol-5-yl)pyridazin-4(1H)-one (**27c**).* Compound **27c** was obtained (66%) as a white solid in a manner similar to that described for the synthesis of **26**; mp 117−118 °C. ^{1}H NMR ($CDCl_3$) δ 3.90 (3H, s), 6.43 (1H, t, J = 8.7 Hz), 6.85−6.90 (1H, m), 7.09 (1H, dd, J = 11.5, 1.7 Hz), 7.34 (1H, d, J = 1.9 Hz), 7.35−7.47 (5H, m), 7.77 (1H, d, J = 2.3 Hz), 7.78 (1H, d, J = 1.9 Hz). LC-MS (ESI) m/z 447 $[M + H]^+$. Anal. Calcd for $C_{21}H_{14}F_4N_4O_3$: C, 56.51; H, 3.16; N, 12.55. Found: C, 56.51; H, 3.14; N, 12.61.

*1-[2-Fluoro-4-(morpholin-4-yl)phenyl]-5-methoxy-3-(1-phenyl-1H-pyrazol-5-yl)pyridazin-4(1H)-one (**27d**).* A suspension of **26** (244 mg, 0.5 mmol), morpholine (0.053 mL, 0.6 mmol), $Pd_2(dba)_3$ (18.3 mg, 0.02 mmol), Xantphos (46.3 mg, 0.08 mmol), and NaO*t*-Bu (67.3 mg, 0.7 mmol) in 1,4-dioxane (2.5 mL) was stirred at 90 °C for 2 h under Ar atmosphere. The mixture was poured into water and extracted with EtOAc. The organic layer was washed with brine, dried over $MgSO_4$, and concentrated under reduced pressure. The residue was purified by column chromatography (basic silica gel, EtOAc) followed by recrystallization from MeOH/water to give **27d** (148 mg, 66%) as an off-white solid; mp 226−228 °C. ^{1}H NMR ($CDCl_3$) δ 3.16−3.19 (4H, m), 3.83−3.87 (4H, m), 3.89 (3H, s), 6.31 (1H, t, J = 9.0 Hz), 6.45 (1H, dd, J = 9.0, 2.6 Hz), 6.58 (1H, dd, J = 14.7, 2.6 Hz), 7.26 (1H, d, J = 1.9 Hz), 7.33−7.45 (5H, m), 7.74 (1H, d, J = 2.3 Hz), 7.77 (1H, d, J = 1.9 Hz). LC-MS (ESI) m/z 448 $[M + H]^+$. Anal. Calcd for $C_{24}H_{22}FN_5O_3$: C, 64.42; H, 4.96; N, 15.65. Found: C, 64.33; H, 4.98; N, 15.59.

*4-{3-Fluoro-4-[5-methoxy-4-oxo-3-(1-phenyl-1H-pyrazol-5-yl)-pyridazin-1(4H)-yl]phenyl}morpholin-3-one (**27e**).* A suspension of **26** (244 mg, 0.5 mmol), 3-morpholinone (60.7 mg, 0.6 mmol), CuI (9.5 mg, 0.05 mmol), *trans*-1,2-diaminocyclohexane (0.012 mL, 0.1 mmol), and K_3PO_4 (212 mg, 1.0 mmol) in 1,4-dioxane (2 mL) was refluxed for 6 h under Ar atmosphere. The mixture was poured into water and extracted with EtOAc. The organic layer was washed with brine, dried over $MgSO_4$, and concentrated under reduced pressure. The residue was purified by column chromatography (basic silica gel, EtOAc) followed by recrystallization from MeOH/water to give **27e** (136 mg, 59%) as a white solid; mp 193−195 °C. ^{1}H NMR ($CDCl_3$) δ 3.75−3.79 (2H, m), 3.90 (3H, s), 4.04−4.07 (2H, m), 4.35 (2H, s), 6.41 (1H, t, J = 9.0 Hz), 7.00 (1H, ddd, J = 9.0, 2.3, 1.1 Hz), 7.31 (1H, d, J = 2.3 Hz), 7.33−7.46 (6H, m), 7.78−7.80 (2H, m). LC-MS (ESI) m/z 462 $[M + H]^+$. Anal. Calcd for $C_{24}H_{20}FN_5O_4$: C, 62.47; H, 4.37; N, 15.18. Found: C, 62.31; H, 4.33; N, 15.25.

*1-[2-Fluoro-4-(2-oxo-1,3-oxazolidin-3-yl)phenyl]-5-methoxy-3-(1-phenyl-1H-pyrazol-5-yl)pyridazin-4(1H)-one (**27f**).* Compound **27f** was obtained (71%) as a pale-yellow solid in a manner similar to that described for the synthesis of **27e**; mp 218−220 °C. ^{1}H NMR ($CDCl_3$) δ 3.90 (3H, s), 4.03−4.08 (2H, m), 4.51−4.56 (2H, m), 6.42 (1H, t, J = 9.0 Hz), 7.01 (1H, ddd, J = 9.0, 2.3, 1.1 Hz), 7.30 (1H, d, J = 1.9 Hz), 7.35−7.45 (5H, m), 7.66 (1H, dd, J = 13.6, 2.3 Hz), 7.78 (2H, d, J = 1.9 Hz). LC-MS (ESI) m/z 448 $[M + H]^+$. Anal. Calcd for $C_{23}H_{18}FN_5O_4$: C, 61.74; H, 4.06; N, 15.65. Found: C, 61.48; H, 4.07; N, 15.54

*1-[2-Fluoro-4-(1H-imidazol-1-yl)phenyl]-5-methoxy-3-(1-phenyl-1H-pyrazol-5-yl)pyridazin-4(1H)-one (**27g**).* Compound **27g** was obtained (8%) as a white solid in a manner similar to that described for the synthesis of **27e**; mp 235−236 °C. ^{1}H NMR ($CDCl_3$) δ 3.93 (3H, s), 6.49 (1H, t, J = 8.7 Hz), 7.03 (1H, ddd, J = 8.7, 2.3, 1.1 Hz), 7.22−7.27 (3H, m), 7.35 (1H, d, J = 1.9 Hz), 7.38−7.49 (5H, m), 7.80 (1H, d, J = 1.9 Hz), 7.82 (1H, d, J = 2.6 Hz), 7.86 (1H, t, J = 1.1 Hz). LC-MS (ESI) m/z 429 $[M + H]^+$. Anal. Calcd for $C_{23}H_{17}FN_6O_2$: C, 64.48; H, 4.00; N, 19.62. Found: C, 64.35; H, 3.90; N, 19.43.

*1-[2-Fluoro-4-(1H-pyrazol-1-yl)phenyl]-5-methoxy-3-(1-phenyl-1H-pyrazol-5-yl)pyridazin-4(1H)-one (**27h**).* A suspension of **26** (4.88 g, 10 mmol), pyrazole (0.681 g, 10 mmol), Cu_2O (0.143 g, 1 mmol), salicylaldoxime (0.549 g, 4 mmol), and Cs_2CO_3 (6.52 g, 20 mmol) in CH_3CN (100 mL) was refluxed for 5 h under Ar atmosphere. The mixture was poured into water and extracted with EtOAc. The organic layer was washed with brine, dried over $MgSO_4$, and concentrated under reduced pressure. The residue was purified by column chromatography (basic silica gel, 33:67 hexane/THF) followed by recrystallization from EtOH/water to give **27h** (1.90 g, 44%) as a pale-yellow solid; mp 214−216 °C. ^{1}H NMR ($CDCl_3$) δ 3.92 (3H, s), 6.44 (1H, t, J = 9.0 Hz), 6.53 (1H, dd, J = 2.3, 1.9 Hz), 7.30 (1H, ddd, J = 9.0, 2.3, 1.1 Hz), 7.34 (1H, d, J = 1.9 Hz), 7.37−7.48 (5H, m), 7.61 (1H, dd, J = 12.4, 2.3 Hz), 7.76 (1H, d, J = 1.9 Hz), 7.79 (1H, d, J = 1.9 Hz), 7.82 (1H, d, J = 2.3 Hz), 7.92 (1H, d, J = 2.3 Hz). LC-MS (ESI) m/z 429 $[M + H]^+$. Anal. Calcd for $C_{23}H_{17}FN_6O_2$: C, 64.48; H, 4.00; N, 19.62. Found: C, 64.41; H, 4.00; N, 19.54.

*Methyl 2-[(4-Iodophenyl)hydrazono]-4-methoxy-3-oxobutanoate (**29**).* Compound **29** was obtained (78%) as a yellow−brown solid in a manner similar to that described for the synthesis of **15**. ^{1}H NMR ($CDCl_3$) δ 3.50 (3H, s), 3.92 (3H, s), 4.64 (2H, s), 7.05−7.10 (2H, m), 7.68−7.73 (2H, m), 12.91 (1H, s).

*Methyl 1-(4-Iodophenyl)-5-methoxy-4-oxo-1,4-dihydropyridazine-3-carboxylate (**30**).* A mixture of **29** (10.0 g, 26.6 mmol), DMFDMA (50 mL), and CH_3CN (50 mL) was refluxed for 2 h. The mixture was concentrated to half its volume under reduced pressure. The precipitate was collected by filtration and washed with EtOAc. The filtrate was concentrated under reduced pressure, and the residue was washed with EtOAc/MeOH (9/1). The combined solid was dried at 60 °C under reduced pressure to give **30** (7.2 g, 70%) as a beige solid. ^{1}H

dx.doi.org/10.1021/jm5013648 | J. Med. Chem. XXXX, XXX, XXX−XXX

NMR ($CDCl_3$) δ 3.96 (3H, s), 3.97 (3H, s), 7.38 (2H, d, J = 9.0 Hz), 7.86 (2H, d, J = 9.0 Hz), 7.90 (1H, s).

*1-(4-Iodophenyl)-5-methoxy-4-oxo-1,4-dihydropyridazine-3-carboxylic Acid (**31**).* Compound **31** was obtained (97%) as a brown solid in a manner similar to that described for the synthesis of **7**. ^{1}H NMR (DMSO-d_6) δ 3.97 (3H, s), 7.69 (2H, d, J = 9.0 Hz), 8.02 (2H, d, J = 9.0 Hz), 8.90 (1H, s), 15.10 (1H, brs).

*3-Acetyl-1-(4-iodophenyl)-5-methoxypyridazin-4(1H)-one (**33**).* A solution of **31** (1.00 g, 2.69 mmol), Meldrum's acid (0.387 g, 2.69 mmol), WSC·HCl (0.515 g, 2.69 mmol), and DMAP (0.328 g, 2.69 mmol) in DMF (10 mL) was stirred at rt for 3 d. The mixture was diluted with brine, acidified with 1 M HCl aq (3 mL), and extracted with EtOAc. The organic layer was dried over $MgSO_4$ and concentrated under reduced pressure to give **32**.

A mixture of **32**, AcOH (10 mL), and water (10 mL) was refluxed overnight. The mixture was concentrated under reduced pressure, and the residue was partitioned between EtOAc and water. The organic layer was dried over $MgSO_4$, passed through a silica gel pad, and concentrated under reduced pressure to give **33** (0.37 g, 37%) as a yellow solid. ^{1}H NMR ($CDCl_3$) δ 2.69 (3H, s), 3.95 (3H, s), 7.39 (2H, d, J = 9.0 Hz), 7.82−7.91 (3H, m).

*1-(4-Iodophenyl)-5-methoxy-3-(1-phenyl-1H-pyrazol-5-yl)-pyridazin-4(1H)-one (**34**).* A mixture of **33** (370 mg, 1.0 mmol), DMFDMA (2 mL), and CH_3CN (5 mL) was refluxed for 1 h. After cooling to rt, the mixture was concentrated under reduced pressure.

To a suspension of the residue in EtOH (10 mL) was added dropwise a solution of phenylhydrazine (0.109 mL, 1.1 mmol) and TFA (1 mL) in EtOH (9 mL) at 0 °C. After stirring at rt overnight, the mixture was concentrated under reduced pressure. The residue was washed with EtOAc to give **34** (170 mg, 36%) as a yellow solid. The washing was concentrated under reduced pressure, and the residue was purified by column chromatography (basic silica gel, 90:10 hexane/EtOAc to 30:70 hexane/EtOAc) to give an additional crop of **34** (65 mg, 14%) as a yellow solid. ^{1}H NMR (DMSO-d_6) δ 3.87 (3H, s), 6.97 (2H, d, J = 9.1 Hz), 7.15 (1H, d, J = 1.9 Hz), 7.33−7.38 (2H, m), 7.42−7.51 (3H, m), 7.72 (2H, d, J = 9.1 Hz), 7.80 (1H, d, J = 1.9 Hz), 8.54 (1H, s).

*5-Methoxy-3-(1-phenyl-1H-pyrazol-5-yl)-1-[4-(1H-pyrazol-1-yl)-phenyl]pyridazin-4(1H)-one (**35**).* Compound **35** was obtained (14%) as a yellow solid in a manner similar to that described for the synthesis of **27h**; mp 218−219 °C. ^{1}H NMR (DMSO-d_6) δ 3.90 (3H, s), 6.59 (1H, s), 7.17 (1H, d, J = 1.5 Hz), 7.29 (2H, d, J = 8.7 Hz), 7.35−7.42 (2H, m), 7.46−7.51 (3H, m), 7.75−7.87 (4H, m), 8.60 (2H, s). LC-MS (ESI) m/z 411 $[M + H]^+$. Anal. Calcd for $C_{23}H_{18}N_6O_2$: C, 67.31; H, 4.42; N, 20.48. Found: C, 67.02; H, 4.46; N, 20.36.

Expression, Purification, Crystallization, and Structure Determination. Human PDE10A catalytic domain (residues 442−779) for crystallographic study was prepared as a fusion protein to SUMO (LifeSensors). The SUMO-PDE10A protein was cloned into a pET-15b vector to acquire a 6× histidine tag at the N-terminus. The histidine-tagged SUMO-PDE10A fused protein was expressed in Rosetta (DE3) pLysS cells (Novagen). Following the addition of 1 mM IPTG, the cells were grown at 24 °C for 5 h. Harvested cells were lysed with lysozyme, followed by microfluidization at 150 MPa. Cell debris was removed by centrifugation at 21612g for 30 min, and the supernatant was incubated with Ni-NTA resin. The PDE10A bound resin was washed with a wash buffer (50 mM Tris-HCl (pH 8.0), 10% glycerol, 300 mM NaCl, and 20 mM imidazole) and eluted with the wash buffer containing 250 mM imidazole. The eluted histidine-tagged SUMO-PDE10A catalytic domain was further purified on a Superdex 200 column in TBS (pH 7.4), 0.5 mM DTT, 1 mM EDTA, and 10% glycerol as a basal buffer. After SUMO cleavage with SUMO protease, the digested protein sample was passed through a Ni-NTA column to remove histidine-tagged SUMO fragment, followed by size-exclusion chromatography using a Superdex 200 column in the basal buffer. Subsequently, the purified catalytic domain was further treated with a mono Q column at pH 8.0 and followed by buffer exchange to the basal buffer by a Sephadex G25. The purified PDE10A catalytic domain was concentrated by ultrafiltration to approximately 19.5 mg/mL and stored at −80 °C until use. Crystals were obtained using the sitting-drop vapor-diffusion method by mixing 50 nL of protein solution (5−10 mg/mL PDE10A catalytic domain in TBS (pH 7.4), 0.5 mM DTT, 1 mM EDTA, and 10% glycerol) and 50 nL of reservoir solution containing 0.1 M HEPES (pH 7.5−8.0), 24−32% PEG 3350, and 200 mM $MgCl_2$ at 4 °C. Complex crystals were obtained by immersing apo crystals into the corresponding reservoir solution containing 0.075 mM inhibitor for 3 days. Prior to data collection, complex crystals were treated with the reservoir solution containing 25% ethylene glycol as a cryoprotectant and were flash-frozen in liquid nitrogen. Diffraction data were collected from a single crystal at the Advanced Light Source beamline 5.0.3 (Berkeley, CA) for compounds **1** and **27h** and BL41XU at SPring-8 (Harima, Japan) for compound **20a** and processed using the program HKL2000.[38] The structures were determined by molecular replacement using MOLREP,[39] utilizing the previously reported coordinate of PDE10A with the PDB accession code 2OUN.[30] Subsequently, the structures were refined through an iterative procedure utilizing REFMAC[40] followed by model building with WinCoot.[41] The dictionary files for the inhibitors were prepared using AFITT (OpenEye Scientific Software).

Enzyme Assay Protocol. Human PDE1A, 3A, 4D2, 5A1, 7B, 8A1, 9A2, and 11A4 enzymes were purchased from BPS Bioscience. Human PDE6AB enzyme was purchased from Scottish Biomedical. Human PDE2A3 was generated from Sf9 transfected with the full-length gene in-house. Human PDE10A2 was generated from COS-7 cells transfected with the full-length gene. The enzymes were stored at −70 °C until use. PDE activities were measured using an SPA (PerkinElmer). To evaluate the inhibitory activity, 10 μL of serial diluted compounds were incubated with 20 μL of PDE enzyme except for PDE1A in assay buffer (50 mM HEPES-NaOH, 8.3 mM $MgCl_2$, 1.7 mM EGTA, and 0.1% bovine serum albumin (BSA) (pH 7.4)) for 30 min at rt. PDE1A enzyme assay was performed in assay buffer (50 mM Tris-HCl, 8.3 mM $MgCl_2$, 0.2 mM $CaCl_2$, 0.1% BSA, and 30 nM Calmodulin (pH 7.5)). Final concentration of DMSO in the assay was 1% as compounds were tested in duplicate or triplicate in 96-well half-area plates (Corning). To start the reaction, 10 μL of substrate [^{3}H]cGMP (PerkinElmer) for PDE1A, 2A3, 5A1, 6AB, 9A2, 10A2, and 11A4 or [^{3}H]cAMP (PerkinElmer) for PDE3A, 4D2, 7B, and 8A1 was added for a final assay volume of 40 μL. After 60 min incubation at rt, 20 μL of 20 mg/mL yttrium SPA beads containing $ZnSO_4$ was added to terminate the PDE reaction. After being settled for more than 120 min, the assay plate was counted in a scintillation counter (PerkinElmer) to allow calculation of inhibition rate. Inhibition rate was calculated on the basis of 0% control wells with DMSO and 100% control wells with enzyme plus 10 μM papaverine (Wako Pure Chemical Industries) for PDE10A2 or without enzymes for the other PDEs. IC_{50} values were determined by logistic curve fitting using nonlinear least-squares regression analysis. The calculation was carried out using either SAS System (SAS Institute Inc., Cary, NC, USA) for compound **27h** or XLfit software (IDBS, Guildford, UK) for the other compounds. Counterscreening of the activity of compound **27h** against a panel of 96 ion channels, receptors, and enzymes was performed at MDS Pharma Services (now Ricerca Biosciences, Taipei, Taiwan), in which compound **27h** was evaluated for its percentage activity at 10 μM.

Metabolic Clearance Assay. In vitro oxidative metabolic studies of the tested compounds were carried out using hepatic microsomes obtained from humans. The reaction mixture with a final volume of 0.05 mL consists of 0.2 mg/mL hepatic microsome in 50 mM KH_2PO_4−K_2HPO_4 phosphate buffer (pH 7.4) and 1 μM test compound. The reaction was initiated by the addition of an NADPH-generating system containing 50 mM $MgCl_2$, 50 mM glucose 6-phosphate, 5 mM β-$NADP^+$, and 15 unit/mL glucose 6-phosphate dehydrogenase at 10% volume of reaction mixture. After the addition of the NADPH-generating system, the mixture was incubated at 37 °C for 0, 15, and 30 min. The reaction was terminated by the addition of an equivalent volume of CH_3CN. After the samples were mixed and centrifuged, the supernatant fractions were analyzed using liquid chromatography tandem mass spectrometry. For metabolic clearance determinations, chromatograms were analyzed for parent compound disappearance rate from the reaction mixtures. All incubations were made in duplicate.

Transcellular Transport Study Using Transporter-Expression System. Human MDR1-expressing LLC-PK1 cells were cultured with minor modification as reported previously.[42] The transcellular transport

dx.doi.org/10.1021/jm5013648 | J. Med. Chem. XXXX, XXX, XXX−XXX

study was performed as reported previously.[43] In brief, the cells were grown for 7 days in HTS Transwell 96-well permeable support (pore size 0.4 μm, 0.143 cm^2 surface area) with polyethylene terephthalate membrane (Corning Life Sciences, Lowell, MA, USA) at a density of 1.125×10^5 cells/well. The cells were preincubated with M199 at 37 °C for 30 min. Subsequently, transcellular transport was initiated by the addition of M199 either to apical compartments (75 μL) or to the basolateral compartments (250 μL) containing 10 μM digoxin, 200 μM lucifer yellow as a marker for the tightness of monolayer, and 10 μM test compounds and terminated by the removal of each assay plate after 2 h. The aliquots (25 μL) in the opposite compartments were mixed with CH_3CN containing alprenolol and diclofenac as an internal standard and then centrifuged. The supernatants were diluted with 10 mM ammonium formate/formic acid (500:1, v/v) and measured in a LC-MS/MS analysis (API4000, AB SCIEX, Foster City, CA, USA). The apparent permeability (P_{app}) of test compounds in the receiver wells was determined and the efflux ratio (ER) for MDR1 membrane permeability test was calculated using the following equation:

$$ER = P_{app,BtoA}/P_{app,AtoB}$$

where $P_{app,AtoB}$ is the apical-to-basal passive permeability-surface area product and $P_{app,BtoA}$ is the basal-to-apical passive permeability-surface area product.

Brain and Plasma Concentration in Mice. Compound **27h** was administered orally to Jcl: ICR mice (male, non-fasted, 8-week old) at 0.3 mg/kg. Blood and brain samples were collected at 0.25, 0.5, 1, 2, 4, 8, and 24 h after oral administration. The blood samples were centrifuged to obtain the plasma fraction. The brain samples were homogenized in saline to obtain the brain homogenate. The plasma and brain homogenate samples were deproteinized with CH_3CN containing an internal standard.

After centrifugation, the supernatants were diluted with the mobile phase (10 mM ammonium formate/CH_3CN/formic acid = 70/30/0.2 (v/v)) and centrifuged again. The compound concentrations in the supernatant were measured by LC/MS/MS with an API5000 triple quadrupole mass spectrometer (AB Sciex).

Measurement of Cyclic Nucleotide Contents in the Mouse Striatum. *Animals.* Five-week-old male ICR mice were supplied by CLEA Japan Inc. (Tokyo, Japan). The mice were housed in groups of 4/cage in a light-controlled room (12 h light/dark cycle with lights on at 07:00). After at least a one-week acclimation period, six-week-old animals were used for the experiment. The care and use of the animals and the experimental protocols used in this research were approved by the Experimental Animal Care and Use Committee of Takeda Pharmaceutical Company, Ltd.

Measurements. Compound **27h** was suspended in 0.5% (w/v) methylcellulose in distilled water. Male ICR mice were sacrificed by a focused microwave irradiation system MMW-05 (Muromachi Kikai, Tokyo, Japan) 60 min after oral administration of compound **27h** (20 mL/kg body weight for mice). Brain tissues were isolated and then sonicated in 0.5 M HCl aq followed by centrifugation. Concentrations of cyclic nucleotides in the supernatant were measured using enzyme immunoassay kits (Cayman Chemical Company, Ann Arbor, MI).

Effects of Compound 27h on PCP-Induced Hyperlocomotion in Mice. *Animals.* Homozygous PDE10A-knockout and their wild-type littermate mice were purchased from Taconic Farms, Inc. (Hudson, NY) and backcrossed to C57BL/6 background. Sixteen-week-old male animals were used for the experiment. The mice were housed in groups of 4/cage in a light-controlled room (12 h light/dark cycle with lights on at 07:00). Food and water were provided ad libitum. The care and use of the animals and the experimental protocols used in this research were approved by the Experimental Animal Care and Use Committee of Takeda Pharmaceutical Company, Ltd.

Measurements. Compound **27h** was suspended in 0.5% (w/v) methylcellulose in distilled water. Compound **27h** was administered orally (po). PCP hydrochloride (lot no. 010M4010) purchased from Sigma-Aldrich, Inc. (USA) was dissolved in saline and was administered subcutaneously (sc). All compounds were dosed in a volume of 20 mL/kg body weight. Hyperlocomotion was measured using a spontaneous motor analyzer MDC system (BrainScience idea. Co. Ltd., Japan). Mice were placed in locomotor chambers for more than 60 min for habituation. Animals were removed from each chamber and treated with either vehicle or compound **27h** and then quickly returned to the chamber. The following doses were used: 0.1, 0.3, and 1.0 mg/kg, po. Sixty minutes after treatment with compound **27h**, animals were again removed from the chambers and treated with either vehicle (saline) or PCP (5 mg/kg as a salt, sc) and then quickly transferred to the test chamber. Activity counts were recorded in successive 1 min bins, and the total number counts were determined for the 120 min period after PCP administration.

■ ASSOCIATED CONTENT

Supporting Information

X-ray data collection and refinement statistics for the crystal structures of PDE10A in complex with compounds **1**, **20a**, and **27h**. This material is available free of charge via the Internet at http://pubs.acs.org.

Accession Codes

The coordinates of the crystal structures of PDE10A in complex with compounds **1** (3WYK), **20a** (3WYL), and **27h** (3WYM) have been deposited in the Protein Data Bank.

■ AUTHOR INFORMATION

Corresponding Author

*Phone: +81-466-32-4123. E-mail: jun.kunitomo@takeda.com.

Present Address

§JFQuinn Consulting, 133 Jay Street, Albany, New York 12210−1805, United States. E-mail: jquinn@uchicago.edu.

Notes

The authors declare no competing financial interest.

■ ACKNOWLEDGMENTS

We thank Drs. William Paquette and Guangwu Chen (Albany Molecular Research Inc.) for chemical synthesis, Dr. Gyorgy Snell (Takeda California, Inc.) for data collection and processing at the Advanced Light Source, Yumi Hayano for preparation of human PDE10A catalytic domain for crystallographic study, Misae Narita for crystal structure analysis, Dr. Tsuyoshi Ishii for in vitro enzyme assays, and Akina Harada for in vivo experiments. We are also grateful to the staff members at BL41XU of Spring-8 for assistance with data collection. This study was sponsored by Takeda Pharmaceutical Company Limited.

■ ABBREVIATIONS USED

AcOH, acetic acid; $AlMe_3$, trimethylaluminum; APCI, atmospheric pressure chemical ionization; aq, aqueous solution; BSA, bovine serum albumin; cAMP, 3′,5′-cyclic adenosine monophosphate; cGMP, 3′,5′-cyclic guanosine monophosphate; DIPEA, *N*,*N*-diisopropylethylamine; DMAP, 4-(dimethylamino)-pyridine; DME, 1,2-dimethoxyethane; DMF, *N*,*N*-dimethylformamide; DMFDMA, *N*,*N*-dimethylformamide dimethyl acetal; DMSO, dimethyl sulfoxide; DPPA, diphenylphosphoryl azide; DTT, dithiothreitol; EGTA, ethylene glycol tetraacetic acid; ESI, electrospray ionization; Et_3N, triethylamine; EtOAc, ethyl acetate; EtOH, ethanol; HBA, hydrogen-bond acceptor; HEPES, 4-(2-hydroxyethyl)-1-piperazineethanesulfonic acid; HMPA, hexamethylphosphoramide; HOBt·H_2O, 1-hydroxybenzotriazole monohydrate; HPLC, high performance liquid chromatography; HTS, high-throughput screening; IPE, diisopropyl ether; IPTG, isopropyl β-D-1-thiogalactopyranoside; KO, knockout; LC-MS, liquid chromatography−mass spectrometry; MDR1, multidrug resistance protein 1; MED, minimum effective dose; MeMgBr, methylmagnesium bromide; MeOH, methanol;

dx.doi.org/10.1021/jm5013648 | J. Med. Chem. XXXX, XXX, XXX−XXX

mp, melting point; MRT, mean residence time; NADP, nicotinamide adenine dinucleotide phosphate; NaOAc, sodium acetate; NaO*t*-Bu, sodium *tert*-butoxide; Ni-NTA, nickel-nitrilotriacetic acid; NMR, nuclear magnetic resonance; P-gp, P-glycoprotein; PCP, phencyclidine; $Pd_2(dba)_3$, tris-(dibenzylideneacetone)dipalladium(0); $Pd(PPh_3)_4$, tetrakis-(triphenylphosphine)palladium(0); PDB, Protein Data Bank; PDE, phosphodiesterase; PEG, polyethylene glycol; rt, room temperature; SAR, structure−activity relationship; SBDD, structure-based drug design; SPA, scintillation proximity assay; SUMO, small ubiquitin-related modifier; TBS, tris-(hydroxymethyl)aminomethane-buffered saline; TFA, trifluoroacetic acid; THF, tetrahydrofuran; TLC, thin-layer chromatography; TMS, tetramethylsilane; TMSCl, trimethylsilyl chloride; TPSA, topological polar surface area; Tris, tris(hydroxymethyl)-aminomethane; WSC·HCl, *N*-[3-(dimethylamino)propyl]-*N*′-ethylcarbodiimide hydrochloride; Xantphos, 4,5-bis-(diphenylphosphino)-9,9-dimethylxanthene

REFERENCES

(1) Bender, A. T.; Beavo, J. A. Cyclic nucleotide phosphodiesterases: molecular regulation to clinical use. *Pharmacol. Rev.* **2006**, *58*, 488−520.

(2) Beavo, J.; Brunton, L. L. Cyclic nucleotide research—still expanding after half a century. *Nature Rev. Mol. Cell Biol.* **2002**, *3*, 710−718.

(3) Lugnier, C. Cyclic nucleotide phosphodiesterase (PDE) superfamily: a new target for the development of specific therapeutic agents. *Pharmacol. Ther.* **2006**, *109*, 366−398.

(4) Loughney, K.; Snyder, P. B.; Uher, L.; Rosman, G. J.; Ferguson, K.; Florio, V. A. Isolation and characterization of PDE10A, a novel human 3′-5-cyclic nucleotide phosphodiesterase. *Gene* **1999**, *234*, 109−117.

(5) Soderling, S. H.; Bayuga, S. J.; Beavo, J. A. Isolation and characterization of a dual-substrate phosphodiesterase gene family: PDE10A. *Proc. Natl. Acad. Sci. U. S. A.* **1999**, *96*, 7071−7076.

(6) Fujishige, K.; Kotera, J.; Michibata, H.; Yuasa, K.; Takebayashi, S.; Okumura, K.; Omori, K. Cloning and characterization of a novel human phosphodiesterase that hydrolyzes both cAMP and cGMP (PDE10A). *J. Biol. Chem.* **1999**, *274*, 18438−18445.

(7) Fujishige, K.; Kotera, J.; Omori, K. Striatum- and testis-specific phosphodiesterase PDE10A. Isolation and characterization of a rat PDE10A. *Eur. J. Biochem.* **1999**, *266*, 1118−1127.

(8) Seeger, T. F.; Bartlett, B.; Coskran, T. M.; Culp, J. S.; James, L. C.; Krull, D. L.; Lanfear, J.; Ryan, A. M.; Schmidt, C. J.; Strick, C. A.; Varghese, A. H.; Williams, R. D.; Wylie, P. G.; Menniti, F. S. Immunohistochemical localization of PDE10A in the rat brain. *Brain Res.* **2003**, *985*, 113−126.

(9) Barnes, T. D.; Kubota, Y.; Hu, D.; Jin, D. Z.; Graybiel, A. M. Activity of striatal neurons reflects dynamic encoding and recoding of procedural memories. *Nature* **2005**, *437*, 1158−1161.

(10) Yin, H. H.; Mulcare, S. P.; Hilário, M. R. F.; Clouse, E.; Holloway, T.; Davis, M. I.; Hansson, A. C.; Lovinger, D. M.; Costa, R. M. Dynamic reorganization of striatal circuits during the acquisition and consolidation of a skill. *Nature Neurosci.* **2009**, *12*, 333−341.

(11) Chappie, T. A.; Helal, C. J.; Hou, X. Current landscape of phosphodiesterase 10A (PDE10A) inhibition. *J. Med. Chem.* **2012**, *55*, 7299−7331.

(12) Kehler, J. Phosphodiesterase 10A inhibitors: a 2009−2012 patent update. *Expert Opin. Ther. Pat.* **2013**, *23*, 31−45.

(13) Verhoest, P. R.; Chapin, D. S.; Corman, M.; Fonseca, K.; Harms, J. F.; Hou, X.; Marr, E. S.; Menniti, F. S.; Nelson, F.; O'Connor, R.; Pandit, J.; Proulx-LaFrance, C.; Schmidt, A. W.; Schmidt, C. J.; Suiciak, J. A.; Liras, S. Discovery of a novel class of phosphodiesterase 10A inhibitors and identification of clinical candidate 2-[4-(1-methyl-4-pyridin-4-yl-1*H*-pyrazol-3-yl)-phenoxymethyl]-quinoline (PF-2545920) for the treatment of schizophrenia. *J. Med. Chem.* **2009**, *52*, 5188−5196.

(14) Helal, C. J.; Kang, Z.; Hou, X.; Pandit, J.; Chappie, T. A.; Humphrey, J. M.; Marr, E. S.; Fennell, K. F.; Chenard, L. K.; Fox, C.; Schmidt, C. J.; Williams, R. D.; Chapin, D. S.; Siuciak, J.; Lebel, L.; Menniti, F.; Cianfrogna, J.; Fonseca, K. R.; Nelson, F. R.; O'Connor, R.; MacDougall, M.; McDowell, L.; Liras, S. Use of structure-based design to discover a potent, selective, in vivo active phosphodiesterase 10A inhibitor lead series for the treatment of schizophrenia. *J. Med. Chem.* **2011**, *54*, 4536−4547.

(15) Malamas, M. S.; Stange, H.; Schindler, R.; Lankau, H.-J.; Grunwald, C.; Langen, B.; Egerland, U.; Hage, T.; Ni, Y.; Erdei, J.; Fan, K. Y.; Parris, K.; Marquis, K. L.; Grauer, S.; Brennan, J.; Navarra, R.; Graf, R.; Harrison, B. L.; Robichaud, A.; Kronbach, T.; Pangalos, M. N.; Brandon, N. J.; Hoefgen, N. Novel triazines as potent and selective phosphodiesterase 10A inhibitors. *Bioorg. Med. Chem. Lett.* **2012**, *22*, 5876−5884.

(16) Hu, E.; Kunz, R. K.; Chen, N.; Rumfelt, S.; Siegmund, A.; Andrews, K.; Chmait, S.; Zhao, S.; Davis, C.; Chen, H.; Lester-Zeiner, D.; Ma, J.; Biorn, C.; Shi, J.; Porter, A.; Treanor, J.; Allen, J. R. Design, optimization, and biological evaluation of novel keto-benzimidazoles as potent and selective inhibitors of phosphodiesterase 10A (PDE10A). *J. Med. Chem.* **2013**, *56*, 8781−8792.

(17) Hu, E.; Andrews, K.; Chmait, S.; Zhao, X.; Davis, C.; Miller, S.; Hill Della Puppa, G.; Dovlatyan, M.; Chen, H.; Lester-Zeiner, D.; Able, J.; Biorn, C.; Ma, J.; Shi, J.; Treanor, J.; Allen, J. R. Discovery of novel imidazo[4,5-*b*]pyridines as potent and selective inhibitors of phosphodiesterase 10A (PDE10A). *ACS. Med. Chem. Lett.* **2014**, *5*, 700−705.

(18) Asproni, B.; Murineddu, G.; Pau, A.; Pinna, G. A.; Langgård, M.; Christoffersen, C. T.; Nielsen, J.; Kehler, J. Synthesis and SAR study of new phenylimidazole-pyrazolo[1,5-*c*]quinazolines as potent phosphodiesterase 10A inhibitors. *Bioorg. Med. Chem.* **2011**, *19*, 642−649.

(19) Kehler, J.; Ritzen, A.; Langgård, A.; Petersen, S. L.; Farah, M. M.; Bundgaard, C.; Christoffersen, C. T.; Nielsen, J.; Kilburn, J. P. Triazoloquinazolines as a novel class of phosphodiesterase 10A (PDE10A) inhibitors. *Bioorg. Med. Chem. Lett.* **2011**, *21*, 3738−3742.

(20) Kilburn, J. P.; Kehler, J.; Langgård, M.; Erichsen, M. N.; Leth-Petersen, S.; Larsen, M.; Christoffersen, C. T.; Nielsen, J. *N*-Methylanilide and *N*-methylbenzamide derivatives as phosphodiesterase 10A (PDE10A) inhibitors. *Bioorg. Med. Chem. Lett.* **2013**, *21*, 6053−6062.

(21) Bauer, U.; Giordanetto, F.; Bauer, M.; O'Mahony, G.; Johansson, K. E.; Knecht, W.; Hartleib-Geschwindner, J.; Carlsson, E. T.; Enroth, C. Discovery of 4-hydroxy-1,6-naphthyridine-3-carbonitrile derivatives as novel PDE10A inhibitors. *Bioorg. Med. Chem. Lett.* **2012**, *22*, 1944−1948.

(22) Hamaguchi, W.; Masuda, N.; Isomura, M.; Miyamoto, S.; Kikuchi, S.; Amano, Y.; Honbou, K.; Mihara, T.; Watanabe, T. Design and synthesis of novel benzimidazole derivatives as phosphodiesterase 10A inhibitors with reduced CYP1A2 inhibition. *Bioorg. Med. Chem.* **2013**, *21*, 7612−7623.

(23) Chino, A.; Masuda, N.; Amano, Y.; Honbou, K.; Mihara, T.; Yamazaki, M.; Tomishima, M. Novel benzimidazole derivatives as phosphodiesterase 10A (PDE10A) inhibitors with improved metabolic stability. *Bioorg. Med. Chem.* **2014**, *22*, 3515−3526.

(24) Höfgen, N.; Stange, H.; Schindler, R.; Lankau, H.-J.; Grunwald, C.; Langen, B.; Egerland, U.; Tremmel, P.; Pangalos, M. N.; Marquis, K. L.; Hage, T.; Harrison, B. L.; Malamas, M. S.; Brandon, N. J.; Kronbach, T. Discovery of imidazo[1,5-*a*]pyrido[3,2-*e*]pyrazines as a new class of phosphodiesterase 10A inhibitiors. *J. Med. Chem.* **2010**, *53*, 4399−4411.

(25) Malamas, M. S.; Ni, Y.; Erdei, J.; Stange, H.; Schindler, R.; Lankau, H.-J.; Grunwald, C.; Fan, K. Y.; Parris, K.; Langen, B.; Egerland, U.; Hage, T.; Marquis, K. L.; Grauer, S.; Brennan, J.; Navarra, R.; Graf, R.; Harrison, B. L.; Robichaud, A.; Kronbach, T.; Pangalos, M. N.; Hoefgen, N.; Brandon, N. J. Highly potent, selective, and orally active phosphodiesterase 10A inhibitors. *J. Med. Chem.* **2011**, *54*, 7621−7638.

(26) Andersen, O. A.; Schönfeld, D. L.; Toogood-Johnson, I.; Felicetti, B.; Albrecht, C.; Fryatt, T.; Whittaker, M.; Hallett, D.; Barker, J. Cross-linking of protein crystals as an aid in the generation of binary protein−ligand crystal complexes, exemplified by the human PDE10a−papaverine structure. *Acta Crystallogr., Sect. D: Biol. Crystallogr.* **2009**, *65*, 872−874.

(27) Chappie, T. A.; Humphrey, J. M.; Allen, M. P.; Estep, K. G.; Fox, C. B.; Lebel, L. A.; Liras, S.; Marr, E. S.; Menniti, F. S.; Pandit, J.;

Schmidt, C. J.; Tu, M.; Williams, R. D.; Yang, F. V. Discovery of a series of 6,7-dimethoxy-4-pyrrolidylquinazoline PDE10A inhibitors. *J. Med. Chem.* **2007**, *50*, 182−185.
(28) Hu, E.; Kunz, R. K.; Rumfelt, S.; Chen, N.; Bürli, R.; Li, C.; Andrews, K. L.; Zhang, J.; Chmait, S.; Kogan, J.; Lindstrom, M.; Hitchcock, S. A.; Treanor, J. Discovery of potent, selective, and metabolically stable 4-(pyridin-3-yl)cinnolines as novel phosphodiesterase 10A (PDE10A) inhibitors. *Bioorg. Med. Chem. Lett.* **2012**, *22*, 2262−2265.
(29) Ertl, P.; Rohde, B.; Selzer, P. Fast calculation of molecular polar surface area as a sum of fragment-based contributions and its application to the prediction of drug transport properties. *J. Med. Chem.* **2000**, *43*, 3714−3717.
(30) Wang, H.; Liu, Y.; Hou, J.; Zheng, M.; Robinson, H.; Ke, H. Structural insight into substrate specificity of phosphodiesterase 10. *Proc. Natl. Acad. Sci. U. S. A.* **2007**, *104*, 5782−5787.
(31) Siuciak, J. A.; Chapin, D. S.; Harms, J. F.; Lebel, L. A.; McCarthy, S. A.; Chambers, L.; Shrikhande, A.; Wong, S.; Menniti, F. S.; Schmidt, C. J. Inhibition of the striatum-enriched phosphodiesterase PDE10A: a novel approach to the treatment of psychosis. *Neuropharmacology* **2006**, *51*, 386−396.
(32) Moore, H. The role of rodent models in the discovery of new treatments for schizophrenia: updating our strategy. *Schizophr. Bull.* **2010**, *36*, 1066−1072.
(33) Olah, G. A.; Narang, S. C.; Balaram Gupta, B. G.; Malhotra, R. Synthetic methods and reactions. 62. Transformations with chlorotrimethylsilane/sodium iodide, a convenient in situ iodotrimethylsilane reagent. *J. Org. Chem.* **1979**, *44*, 1247−1251.
(34) Chen, Q.-Y.; Wu, S.-W. Methyl fluorosulphonyldifluoroacetate; a new trifluoromethylating agent. *J. Chem. Soc., Chem. Commun.* **1989**, 705−706.
(35) Ali, M. H.; Buchwald, S. L. An improved method for the palladium-catalyzed amination of aryl iodides. *J. Org. Chem.* **2001**, *66*, 2560−2565.
(36) Klapars, A.; Antilla, J. C.; Huang, X.; Buchwald, S. L. A general and efficient copper catalyst for the amidation of aryl halides and the *N*-arylation of nitrogen heterocycles. *J. Am. Chem. Soc.* **2001**, *123*, 7727−7729.
(37) Cristau, H.-J.; Cellier, P. P.; Spindler, J.-F.; Taillefer, M. Mild conditions for copper-catalysed *N*-arylation of pyrazoles. *Eur. J. Org. Chem.* **2004**, 695−709.
(38) Otwinowski, Z.; Minor, W. Processing of X-ray diffraction data collected in oscillation mode. *Methods Enzymol.* **1997**, *276*, 307−326.
(39) Vagin, A.; Teplyakov, A. MOLREP: an automated program for molecular replacement. *J. Appl. Crystallogr.* **1997**, *30*, 1022−1025.
(40) Collaborative Computational Project, Number 4. The CCP4 suite: programs for protein crystallography. *Acta Crystallogr., Sect. D: Biol. Crystallogr.* **1994**, *50*, 760−763.
(41) Emsley, P.; Lohkamp, B.; Scott, W. G.; Cowtan, K. Features and development of *Coot*. *Acta Crystallogr., Sect. D: Biol. Crystallogr.* **2010**, *66*, 486−501.
(42) Sugimoto, H.; Hirabayashi, H.; Kimura, Y.; Furuta, A.; Amano, N.; Moriwaki, T. Quantitative investigation of the impact of P-glycoprotein inhibition on drug transport across blood-brain barrier in rats. *Drug Metab. Dispos.* **2011**, *39*, 8−14.
(43) Takeuchi, T.; Yoshitomi, S.; Higuchi, T.; Ikemoto, K.; Niwa, S.; Ebihara, T.; Katoh, M.; Yokoi, T.; Asahi, S. Establishment and characterization of the transformants stably-expressing *MDR1* derived from various animal species in LLC-PK$_1$. *Pharm. Res.* **2006**, *23*, 1460−1472.